PHOTOPRODUCTION OF POSITIVE K MESONS IN HYDROGEN

Thesis by

Howard M. Brody

In Partial Fulfillment of the Requirements

For the Degree of

Doctor of Philosophy

California Institute of Technology

Pasadena, California

1959

ACKNOWLEDGEMENTS

Dr. R. L. Walker supervised this work and his interest and suggestions have been of great assistance. The help he provided during the author's entire graduate residence cannot be sufficiently acknowledged.

The experiment was performed jointly with Dr. A. M. Wetherell whose assistance was invaluable.

The encouragement and helpful suggestions of Dr. R. F. Bacher are deeply appreciated. Dr. M. Sands, Dr. J. M. Teem and the other members of the staff of the Synchrotron Laboratory offered valuable advice on many occasions.

Mr. F. P. Dixon calibrated much of the equipment and numerous discussions with him were very valuable.

The author would like to thank Dr. V. Z. Peterson and Mr. E. B. Emery for the maintenance of the liquid hydrogen target. The work of Mr. Dan Sell, Mr. Larry Loucks and the synchrotron engineering staff and crew in maintaining the machine and equipment is gratefully acknowledged.

Mr. R. Diebold helped to analyze much of the data and my wife Lois typed the thesis drafts and provided constant encouragement.

The financial support of the U. S. Atomic Energy Commission is gratefully acknowledged.

ABSTRACT

The method of Donoho and Walker (1) for measuring K particle photoproduction has been improved in order to provide a clearer identification of the K mesons and to allow measurements at a more forward angle, 10^{o} in the laboratory. Charged particles produced in a liquid hydrogen target by the bremsstrahlung beam were analyzed by a magnetic spectrometer. The K^{+} particles were identified by a time of flight velocity measurement combined with a measurement of the correlated pulse height in three scintillation counters. A lucite Čerenkov counter was used to veto fast particles (π, μ, and e) and various counters were positioned in the magnetic field to eliminate particles that might scatter off of the pole pieces.

The results obtained are in good agreement with an isotropic angular distribution for the $\gamma + p \rightarrow K^{+} + \Lambda^{o}$ reaction at a photon energy of 1000 MEV and in good agreement with the revised Cornell (2) data at 1010 MEV.

A cross section for the reaction $\gamma + p \rightarrow K^{+} + \Sigma^{o}$ was measured and found to be somewhat smaller than the corresponding Λ^{o} cross section, but the large statistical errors on this one Σ^{o} point make any further analysis difficult.

TABLE OF CONTENTS

SECTION	TITLE	PAGE
ACKNOWLEDGEMENTS		
ABSTRACT		
TABLE OF CONTENTS		
I.	INTRODUCTION	1
II.	EXPERIMENTAL METHOD	7
III.	EQUIPMENT	13
	A. The X-Ray Beam and Hydrogen Target	13
	B. Magnet	19
	C. Scintillation Counters	19
	D. Čerenkov Counter	26
	E. Counters Designed to Eliminate Scattered Particles	34
	F. Time of Flight Circuit	35
	G. Calibrations	50
IV.	EXPERIMENTAL DATA	56
	A. K Identification	56
	B. Backgrounds	77
	C. Counting Rates	78
V.	CROSS SECTIONS AND CORRECTIONS	82
	A. Counting Rate-Cross Section Relationship	82
	B. Decay Correction	84
	C. Other Corrections	87
	D. Cross Sections	89
VI.	THEORY	91
VII.	RESULTS AND CONCLUSIONS	98
APPENDIX		106
REFERENCES		108

INTRODUCTION

In 1935 Yukawa, in attempting to explain nuclear forces, proposed the existence of a strongly interacting particle of short lifetime and mass intermediate between an electron and nucleon. Soon after the μ meson, a particle of short lifetime and intermediate mass was discovered. However further investigations showed that the μ meson could not be considered to be the Yukawa particle because it interacted weakly with nuclear matter. In 1947 the π meson was discovered by Powell and further investigation showed it to have the properties predicted by Yukawa.

In subsequent cosmic ray studies many curious events were observed that could not be explained by any known particle. These events were attributed to new particles that interacted strongly with matter, were produced abundantly, and decayed in times between 10^{-8} and 10^{-10} seconds.

This posed a formidable problem because the characteristic interaction time of strongly interacting particles is of the order of 10^{-20} seconds, while the decay times of these new strongly interacting particles indicated a weak process was taking place.

A solution, suggested by Pais (4) was that these particles could only be produced in pairs (associated production) and this was soon confirmed experimentally.

Gell - Mann and Nishijima (5) then proposed a new quantum number, strangeness (S) which was conserved in all strong (nuclear

and electromagnetic) interactions, but was not conserved in the weak interactions presumably responsible for the decays of these new particles. The Λ, Σ and Ξ hyperons (particles more massive than nucleons) were assigned strangeness -1, -1 and -2 respectively while the K^+, K^o and K^- $\overline{K}^o$ mesons were assigned strangeness +1 and -1 respectively. This scheme allowed K^+ and K^o mesons to be produced in association with the Λ and Σ hyperons and accounted for the observed preponderance of K^+ mesons over K^- mesons.

In addition this theory predicted two new particles, the Σ^o and Ξ^o which have since been discovered.

A great deal of work has gone into determining the properties of these strange particles and numerous experiments have been performed on their production and interaction with matter in an effort to determine the role they play in nuclear forces. No evidence for any violation of strangeness conservation in nuclear interactions has been observed in any of these reactions.

In investigating the interaction of high energy photons with matter much has been learned about the π meson and nuclear forces. It was hoped that if K mesons could be produced by photons, the study of these reactions might provide valuable information about the nature of the strange particles and their mutual interactions.

If the rules of strangeness were violated, K^+ mesons from the reaction $\gamma + p \rightarrow K^+ + n^o$ should be seen at photon energies above 630 MEV. If $\Delta S = 0$ for electromagnetic interactions then a photon energy of 910 MEV is required to obtain K mesons from the reaction $\gamma + p \rightarrow K^+ + \Lambda^o$, and higher energies are required for the reactions involving the Σ hyperons.

The preliminary work on K^+ mesons done by Donoho and Walker (1) in this laboratory has shown that K particles can be produced by high energy photons. An upper limit on the yield for the strangeness violating reaction $\gamma + p \rightarrow K^+ + n^o$ was set at 5 °/o of the yield for the reaction $\gamma + p \rightarrow K^+ + \Lambda^o$. Cross sections were obtained for the latter reaction at several angles and energies using a magnet, three scintillation counters and a time of flight measurement to detect the K mesons. Donoho and Walker were able to obtain an excitation function at 90^o in the center of momentum system which seemed to rise linearly with the K particle momentum, as opposed to a p^3 or a p^5 dependence. However, these results were not conclusive due to the poor statistics obtained.

The angular distributions appeared to deviate from isotropy, but again the statistics made any analysis subject to large uncertainties. In addition there was the possibility of error due to identifying a pion or scattered proton as a K meson, and uncertainties in the efficiency of the time of flight circuit.

The differential cross sections obtained for strange particle production were of the order of 0.15 μ barns/ster, about a factor of

100 below the pion cross sections. This made the experiments difficult due to the low counting rates and the large background from pions and recoil protons.

The purpose of the present experiment was to obtain better statistical accuracy, extend the angular distribution to more forward angles, provide a more positive identification of the K mesons, and obtain information concerning the reaction $\gamma + p \rightarrow K^+ + \Sigma^o$.

Work of a similar nature is being conducted at Cornell University (2). Their angular distribution at 1010 MEV is isotropic, but at 980 MEV it deviates from isotropy at forward angles. The data taken below 1000 MEV are consistant with a linear dependence upon momentum for the cross section, while the points taken at 1006, 1010, 1032 and 1066 MEV have the same cross section well within the statistical accuracy of the experiment.

Cornell has in addition obtained a cross section for the $\gamma + p \rightarrow K^+ + \Sigma^o$ reaction at one point. The value of this cross section is 60 $^o/_o$ of the value of the cross section for the corresponding point of the $\gamma + p \rightarrow K^+ + \Lambda^o$ reaction.

Most of the properties of the strange particles are well known, with the exception of their parity and magnetic moments. The evidence concerning the spin of these particles is very good for an assignment of zero for the K and $\frac{1}{2}$ for the Λ^o. The evidence points toward a spin $\frac{1}{2}$ for the Σ as well, but it is not as strong (6).

The hyperon magnetic moments have been the subject of some theoretical speculation (7) but at present no experiments designed to

measure these moments have been performed.

The evidence concerning the relative K-hyperon parity is very poor, but it does tend to favor the pseudoscalar case over the scalar. It was hoped that the data obtained in this experiment might shed some light on the subject.

The equipment used by Donoho and Walker (1) was modified so as to eliminate most of the pions and scattered protons, a trouble in their experiment, and to allow data to be taken at angles as small as 10^{o} in the lab. In addition, the apparatus was carefully calibrated and continuously monitored to reduce the possibility of errors arising from drift in gains or shifting biases. The equipment consisted of a magnetic spectrometer which focused particles of a given momentum into a system of three scintillation counters, absorbers, and a Čerenkov counter. A counter was placed in the aperture of the magnet to serve as the first signal for a time of flight measurement circuit and, for a portion of the experiment, this counter also defined the solid angle of the spectrometer and eliminated particles which might scatter from the pole faces of the magnet. For the remainder of the experiment a larger counter was placed in the aperture of the magnet and the magnet was lined with a series of thin counters in a manner such that they would produce a signal every time a particle scattered off the pole faces. Because the magnetic field of the spectrometer swept away low momenta particles, it became possible to work at very small forward angles without placing absorbers in front of these aperture counters or having them "jam" because of too high a counting rate.

The results of this experiment are consistent with an isotropic angular distribution at a photon energy of 1000 MEV. The revised Cornell data at 1010 MEV seem to confirm this and agree well with the data obtained in this experiment.

There remains however, a discrepancy due to the low values of the cross section obtained by Cornell at 980 MEV. The disagreement is worse at forward angles where it amounts to almost a factor of two.

The results obtained cannot be interpreted as favoring a scalar or pseudoscalar meson, and further work must be done to obtain information about parity.

Because of the large statistical error on the one Σ point taken, no conclusions about this reaction can be reached, other than noting that the cross section appears somewhat smaller than the cross section of the Λ^{o} point with the same K^{+} momentum in the center of momentum system.

II. EXPERIMENTAL METHOD

The measurement of the differential cross sections for photoproduction of K mesons involves the determination of the number of K particles emitted from a target with a given momentum at a given angle per unit of beam passing through the target.

Since the photoproduction of K^+ mesons in association with Λ^o hyperons is a two body reaction, it is sufficient to measure the angle and momentum of the K meson in order to specify all the other quantities in the kinematics, as long as no other reaction producing K^+ mesons is energetically possible.

This is accomplished by keeping the peak energy of the Synchrotron just above the energy of the photons producing the K mesons being detected.

If the Synchrotron energy is raised somewhat higher, it then becomes possible to detect the K's from reactions such as $\gamma + p \rightarrow K^+ + \Sigma^o$ with reactions like $\gamma + p \rightarrow K^+ + K^- + p$ still energetically forbidden. However, when K particles from the Σ reactions are being detected, K mesons from a Λ^o reaction of a lower photon energy are being observed also, and add to the counting rate.

In order to determine the reaction a specific K^+ meson comes from, information about the photon producing the reaction or information about the other reaction product must be obtained.

The Σ^o hyperon decays into a Λ^o and γ ray in about 10^{-20} seconds, (a theoretical estimate) at which point it very closely

resembles in energy and angle a Λ^{o} from the other possible K^{+} reaction. The Λ^{o} in turn decays quickly (10^{-10} sec.), and there is little hope of discerning one reaction from the other by detecting the Λ^{o} decay products with counters.

The γ ray from the Σ^{o}-Λ^{o} transition is emitted almost isotropically in the lab, and even if it were detected with some reasonable efficiency, photons from sources such as decay of the π^{o} mesons ($\Lambda^{o} \rightarrow n + \pi^{o}$, 37 %) would produce an appreciable background.

The method of determining the photon energy was used successfully by doing the experiment at two energies and then subtracting the counting rates. The major disadvantage of this system is the poor counting statistics obtained when two numbers of comparable magnitudes were subtracted.

A magnet and a series of counters were used to define the angle and momentum of the particles emitted from the target, but the actual identification of the individual K mesons as they pass through the equipment was difficult due to the large number of other particles emitted with the same momentum at the same angle.

At a typical point, the ratio of protons to pions to K mesons counted was 2000:1000:1. With the normal beam intensity, the counting rate for K mesons was several per hour. Because of these two factors, the equipment used to detect the K mesons had to be both very selective and very efficient.

To determine what particle has traversed the system, it is sufficient to identify one of its unique properties such as mass, lifetime,

or decay products. Once the momentum is specified by the magnet and counters, the mass can be determined by a velocity measurement.

To determine the velocity of a charged particle, scintillation counters were used since the energy loss of a particle is a function of its velocity. However, the energy loss of a particle in a counter and the associated conversion of this into useful information are subject to a statistical fluctuation which causes some loss of velocity discrimination. Because of this fluctuation there is a small probability that a pion may be indistinguishable from a K meson on the basis of energy loss. Since there were hundreds of pions per K, if some additional means of discriminating against pions were not used, the K identification would be in considerable error. Donoho and Walker were able to reduce the π to K ratio considerably by the use of a time of flight circuit and then correlate the pulse heights in the three scintillation counters to distinguish the K's from the pions.

In the present experiment a Čerenkov counter has been added to the time of flight to help eliminate the pions and the combined effect of these two devices succeeded in eliminating all but about one per thousand of the minimum ionizing particles passing through the system.

A second difficulty concerned protons of higher momenta which scattered off the pole pieces and through the counters with a velocity similar to that of the K mesons.

In the early part of this experiment these scattered particles were largely eliminated by positioning a narrow counter in the aperture of the magnet and requiring all accepted particles to produce

a signal in this counter. During the later runs, the magnet pole face was lined with scintillating strips which produced a signal when a particle scattered from the pole face.

The block diagram of the electronics used is shown in figure 1. The outputs of the three scintillation counters, the time of flight circuit, and the Čerenkov circuit were fed into a multi-channel discriminator and a coincidence circuit. The output pulse of this circuit was used to trigger an oscilloscope upon which several signals were displayed and to advance the film in a camera which recorded the scope trace.

The signals usually displayed on the oscilloscope were the outputs of the three scintillation counters and the time of flight circuit. Each of these four pulses provided an amplitude which was related in a known manner to the velocity of the particle passing through the equipment. By photographing each trace it was possible to correlate all four signals in an attempt to insure that each event was properly identified. When the anti-scattering counters lining the magnet pole face were in use, their output pulse was displayed on the trace also.

Before and after each K meson run, a pion calibration run was taken by setting the time of flight circuit to the proper delay and placing the Čerenkov circuit in coincidence, not veto. Approximately 100 pion pictures were taken each time and in this way the time of flight circuit and the three scintillation counters were kept under surveillance as to efficiency and shifts in gain. From the data obtained in these calibration runs, pulse height criteria could be set for the K runs.

FIGURE 1

BLOCK DIAGRAM OF ELECTRONICS

"Fans" refer to the anti-scattering counters installed on the pole faces of the magnet.

BLOCK DIAGRAM K^+ ELECTRONICS

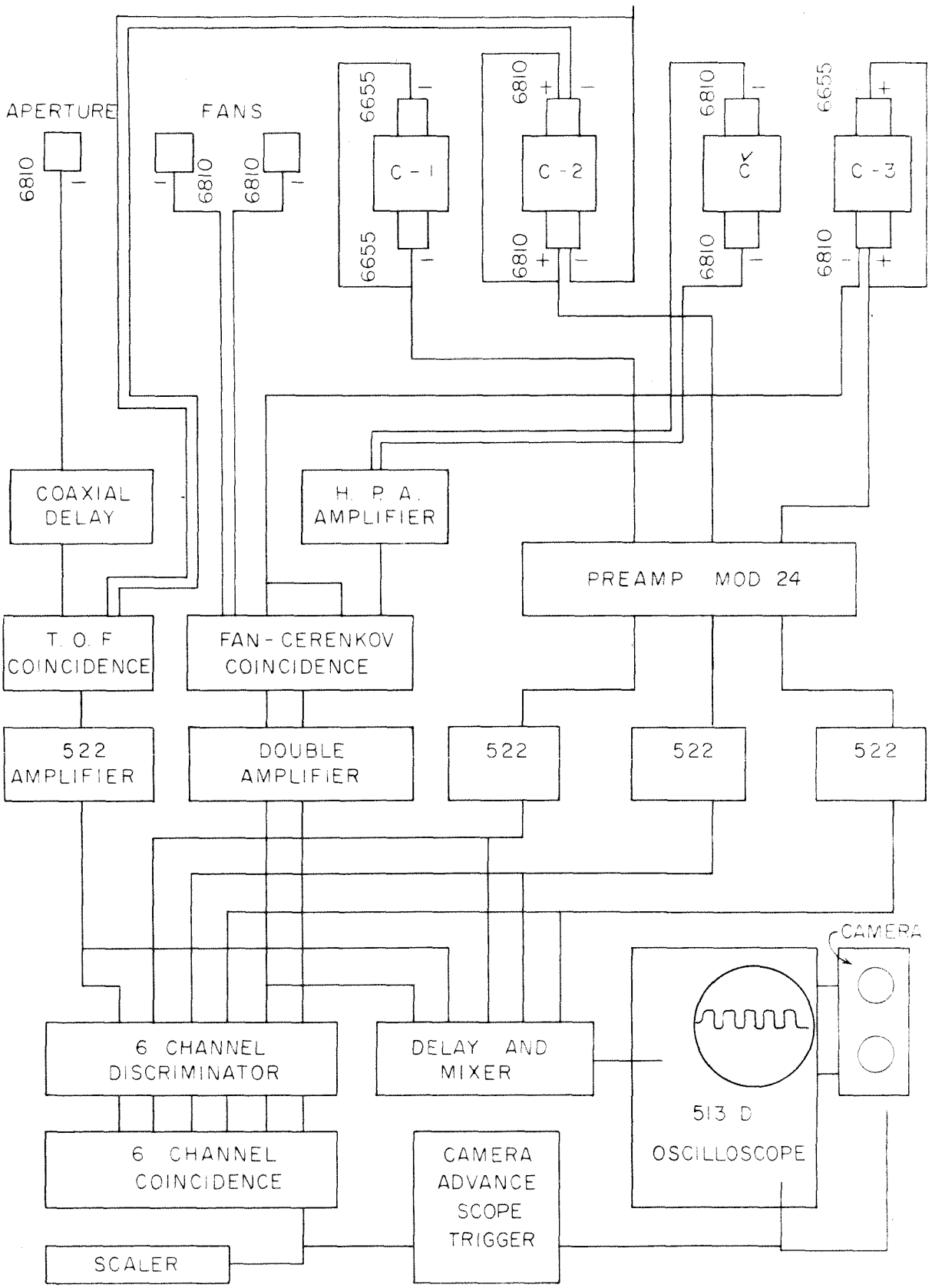

III. EQUIPMENT

A. The X-Ray Beam and Hydrogen Target

The Cal Tech Synchrotron is a circular electron accelerator producing photons of energy up to 1. 1 BEV. The machine is pulsed once a second and the emergent bremsstrahlung beam has an average energy of approximately 10^{11} MEV per pulse. The magnetic field used to contain the electrons rises linearly to a peak field of 14 kilogauss in a quarter of a second, except for a 20 millisecond "plateau" during which it remains constant. During this constant field period the radio frequency accelerating voltage is reduced and the high energy electrons spiral into a radiator of . 2 radiation lengths in thickness, to produce the bremsstrahlung beam. The magnetic field is measured during this plateau period and from this measurement the energy of the electrons striking the radiator is determined.

Upon emerging from the machine, the beam passes through a primary collimator, several scrapers, sweeping fields and targets before striking an ion chamber located in the lead beam catcher (figure 2).

The spectrum of the bremsstrahlung has been measured by Donoho, Emery, and Walker (8) and the value obtained for the peak energy agrees with the magnetic field measurement to about $\frac{1}{2}$ o/o. The spectrum determined the quantity $B(E_o, k/E_o)$ to be equal to 0. 9 in the range of interest in this experiment. $B(E_o, k/E_o)$ is defined by the expression $n(k)\,dk = \frac{W}{E_o} B(E_o k/E_o) \frac{dk}{k}$ where $n(k)\,dk$ is the

FIGURE 2

PLAN VIEW OF EXPERIMENTAL AREA

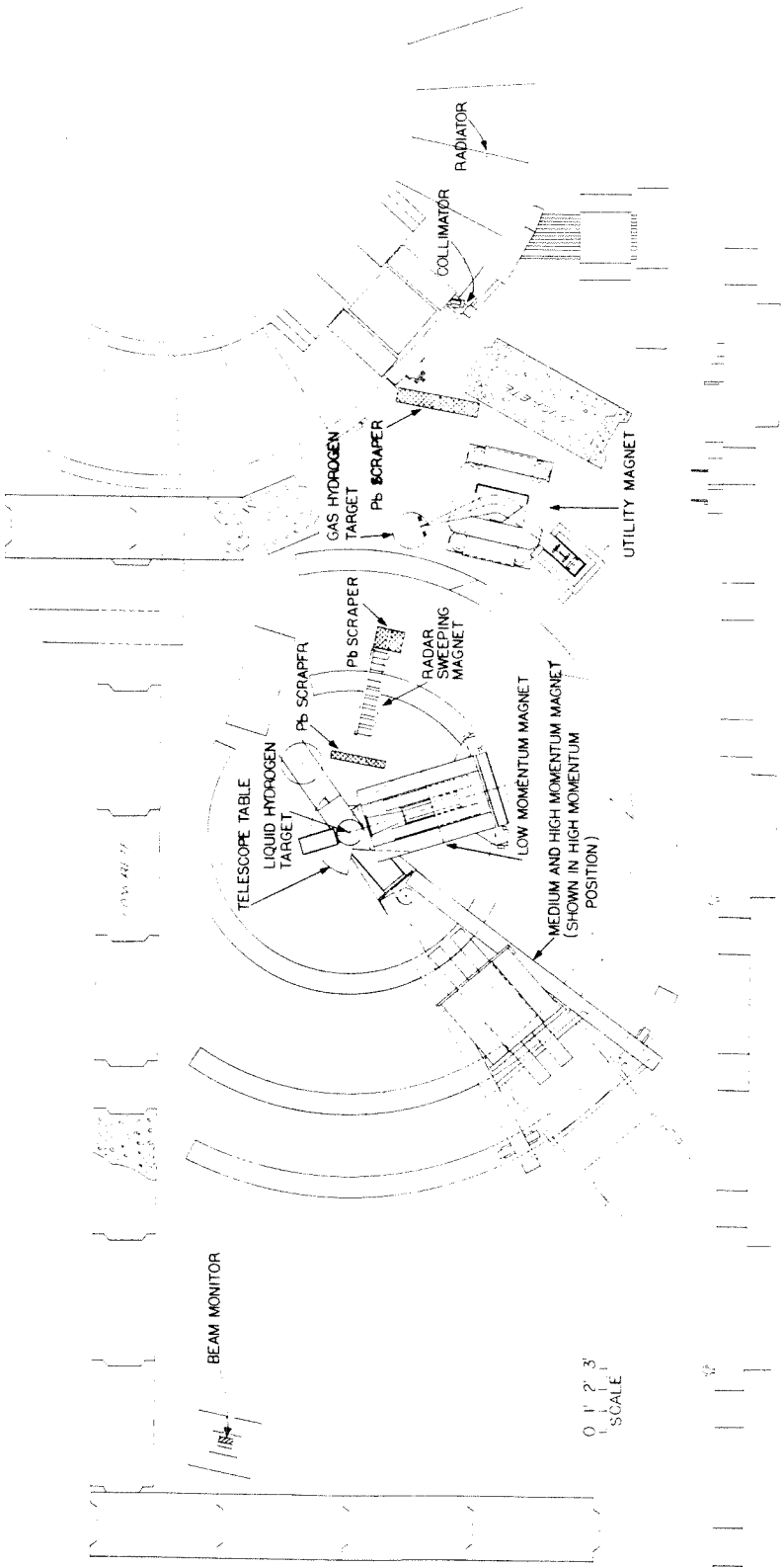
RADIATOR
COLLIMATOR
GAS HYDROGEN TARGET
Pb SCRAPER
UTILITY MAGNET
Pb SCRAPER
RADAR SWEEPING MAGNET
Pb SCRAPER
LIQUID HYDROGEN TARGET
TELESCOPE TABLE
LOW MOMENTUM MAGNET
MEDIUM AND HIGH MOMENTUM MAGNET (SHOWN IN HIGH MOMENTUM POSITION)
BEAM MONITOR
0 1' 2' 3'
SCALE

number of photons in the interval k to k + dk for a beam of total energy W and peak photon energy E_o.

The total energy in the beam, W, was measured by the thick ion chamber which the photons strike. This ion chamber has been calibrated by R. Gomez (9) using a quantameter designed by R. R. Wilson (10). The absolute calibration of the chamber obtained was 4.93×10^{18} D MEV/coulomb at 0° C and 760 mm. Hg.

The value D is the dependence of the chamber upon peak photon energy and is given in table 1.

TABLE I.

Dependence of W on Peak Photon Energy

Peak Energy (MEV)	D
900	1.020
1025	1.063
1072	1.076
1080	1.080
1115	1.090

The charge produced by the ion chamber was measured with a precision integrator which would reset to zero when the charge reached a certain value. Every time the integrator reset, one bip (beam integrator pulse) was recorded.

The integrator was calibrated several times in the course of the experiment. For the initial runs it was $.221 \times 10^{-6}$ coulombs/bip.

For the later runs it was . 218 x 10^{-6} coulombs/bip. The values for W and n(k) corrected for temperature, pressure, energy and the integrator appear in table II.

TABLE II

Value of n(k)

Run	E_o	$W \frac{mev}{bip}$	k	$n(k) = \frac{W}{E_o} B(E_o, k/E_o) \frac{1}{k}$
Initial	900	1.245×10^{12}	1000	$(k > E_o)$
	1072	1.33×10^{12}	1000	1.100×10^{6}
Later	900	1.233×10^{12}	1000	$(k > E_o)$
	1025	1.281×10^{12}	953	1.180×10^{6}
	1080	1.306×10^{12}	1000	1.087×10^{6}
	1115	1.336×10^{12}	1073	1.001×10^{6}

When the runs were taken at 10^{o}, the beam intercepted the magnet and consequently it was necessary, in order to monitor the beam, to mount an ion chamber in front of the magnet. Because of the slight divergence of the beam, the ion chamber on the magnet might have intercepted more of the beam than the ion chamber located in the beam catcher. This effect was measured experimentally using a thin ion chamber as a monitor. For the first set of runs the effect was 2 $^{o}/o$. During the course of the second set of runs, two measurements

were made, each producing a 10 °/o effect. This was repeated later and a 5 °/o effect was measured. The same effect was very carefully checked by Gomez at a later date and he found it to be at most 1 °/o. Since this discrepancy has not been resolved, a value of 5 °/o has been assigned to the two runs (k = 953 MEV, 1073 MEV at 10° lab) with a large error (5 °/o), and a value of 2 °/o to the first run (k = 1000, 10° lab) with a 1 °/o error.

At the 1115 MEV point a fraction of the electron beam spiralled into the radiator before the plateau, and this was monitored by photographing a scope trace displaying the aperture counter dynode voltage and the magnitude of the magnetic field. Since the time constant of the dynode was long compared to the beam pulse, the fraction of beam radiated at any time was the ratio of the dynode voltage shift at that time to the total shift in dynode voltage. This early beam dump decreased the counting rate at this point by approximately 13 °/o.

The hydrogen target used in this experiment was designed by V. Z. Peterson and a simplified drawing of it appears in figure 3. The liquid hydrogen was contained in a thin walled mylar cylinder (the appendix) 3" in diameter. Concentrically around the cylinder were several very thin foil radiation shields and a thick (25 mil) mylar wall as the outside wall of the vacuum system. The width of photon beam was $4\frac{1}{2}$ cm. and the height was $5\frac{1}{2}$ cm. when it passed through the target. By measuring the beam density distribution at the target by photographic means, the effective target length was determined to be 7. 23 cm.

B. Magnet

The magnetic spectrometer used in this experiment had a wedge shaped uniform field and was capable of focusing particles up to a momentum of 600 MEV/C. The path length between foci was 165 inches and the momentum dispersion, $\frac{\Delta P}{P_o} = .10$, was fixed by the width of a scintillation counter placed near the rear focus. The value of the magnetic field could be determined to 0.1 per cent by lowering a proton resonance probe into the magnetic field.

The nominal solid angle, .00785 ster., the central momentum, P_o, and the momentum dispersion, $\frac{\Delta P}{P_o}$ were determined by the use of a floating wire technique. These measurements and other properties of the spectrometer are described in a Synchrotron Lab report written by P. L. Donoho (11) and revised by F. P. Dixon. A cross sectional view taken through the median plane is shown in figure 3.

The effective solid angle of the magnet was changed by the positioning of various counters, and this will be described in a later section.

C. Scintillation Counters

There were three large scintillation counters placed inside the lead and steel counter housing at the focus of the magnet. They consisted of rectangular slabs of polystyrene base plastic scintillator with two lucite light pipes glued on the ends. A phototube viewed each lightpipe and the tubes were placed in concentric mumetal, Fernetic Co-Netic and soft iron cylinders, to prevent the magnetic field of the

FIGURE 3

EXPERIMENTAL ARRANGEMENT

A cross-sectional view taken through the median plane of the magnet.

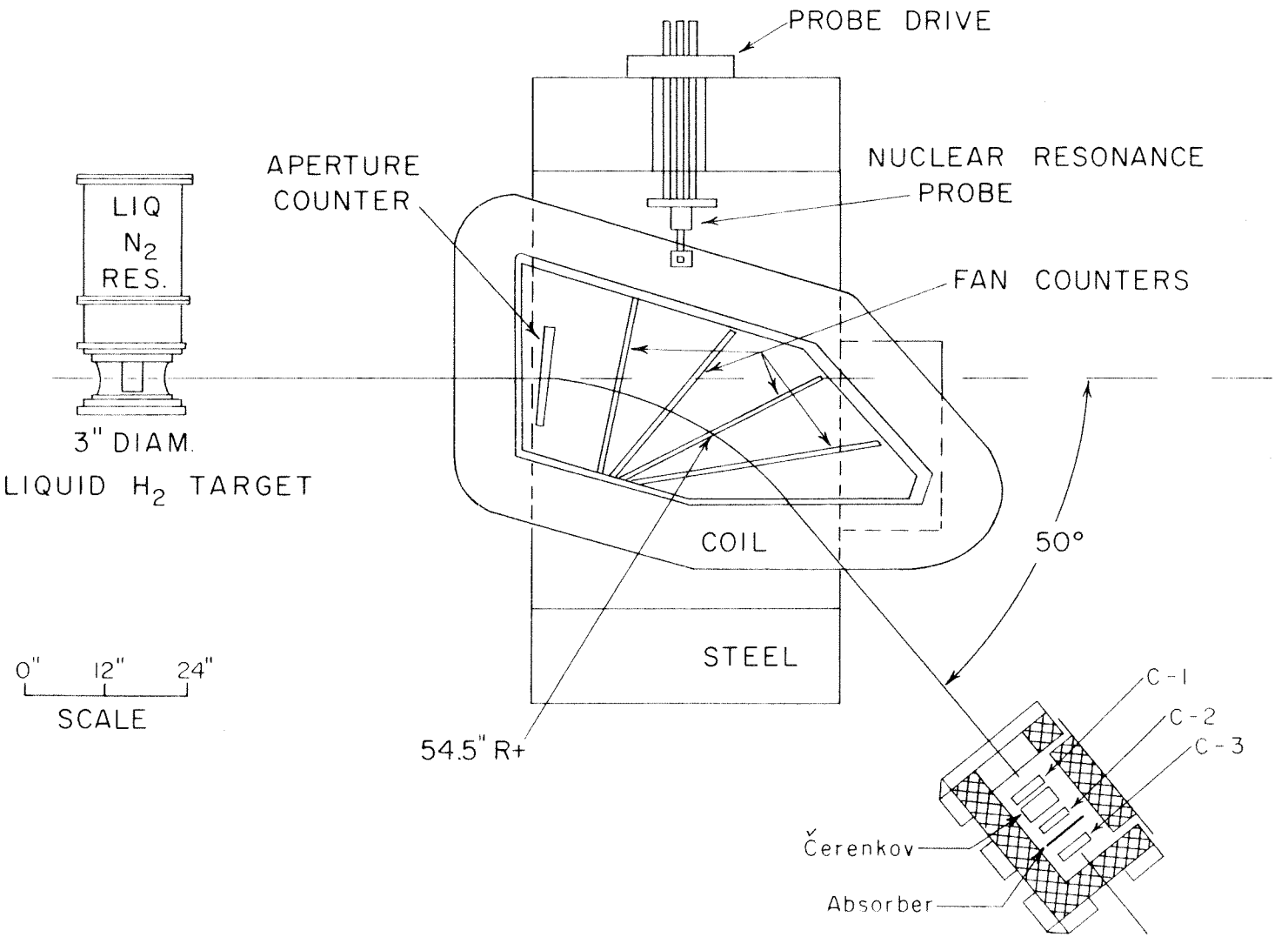
PROBE DRIVE
APERTURE COUNTER
NUCLEAR RESONANCE PROBE
FAN COUNTERS
LIQ N_2 RES.
3" DIAM.
LIQUID H_2 TARGET
COIL
STEEL
50°
0" 12" 24"
SCALE
54.5" R+
C-1
C-2
C-3
Čerenkov
Absorber

spectrometer from reducing their gain. The magnetic and electrostatic shielding is shown in figure 4. Table III describes the counters.

TABLE III

Description of Scintillation Counters

Counter	Scintillator Size (Inches)	Photomultiplier Tubes Used
C-1	5.75x10x0.78	2 RCA-6655
C-2	4.75x11x0.78	2 RCA-6810A
C-3	5.75x11x0.39	1 RCA-6655
		1 RCA-6810

The RCA 6810 tubes were used where large signals were needed to drive fast coincidence circuits without the use of additional amplifiers.

The "slow" signals from the two tubes on each counter were added and shaped in a preamplifier mounted on the magnet frame. The resultant shaped pulses were amplified and fed into a six channel gated discriminator and then a slow (.15μsec.) coincidence circuit. After amplification the pulses were also fed into a delay and mixing network so that they might be displayed on an oscilloscope.

The signal produced by a scintillation counter is proportional to the energy a particle loses in traversing the counter. This would provide a good measure of the particle velocity if the counter resolution were perfect, and if there were no statistical fluctuations in the energy loss.

FIGURE 4

MAGNETIC AND ELECTROSTATIC SHIELDING

OF RCA 6810 PHOTOTUBES

The tube is wrapped in a thin aluminum foil (not shown here) to act as an electrostatic shielding. This foil, the mumetal cylinder, and the metal collar are raised to a high potential by the thin wire which is connected to pin No. 1.

In the tube base pin No. 1 is connected to the cathode voltage by a 10 MEG resistor.

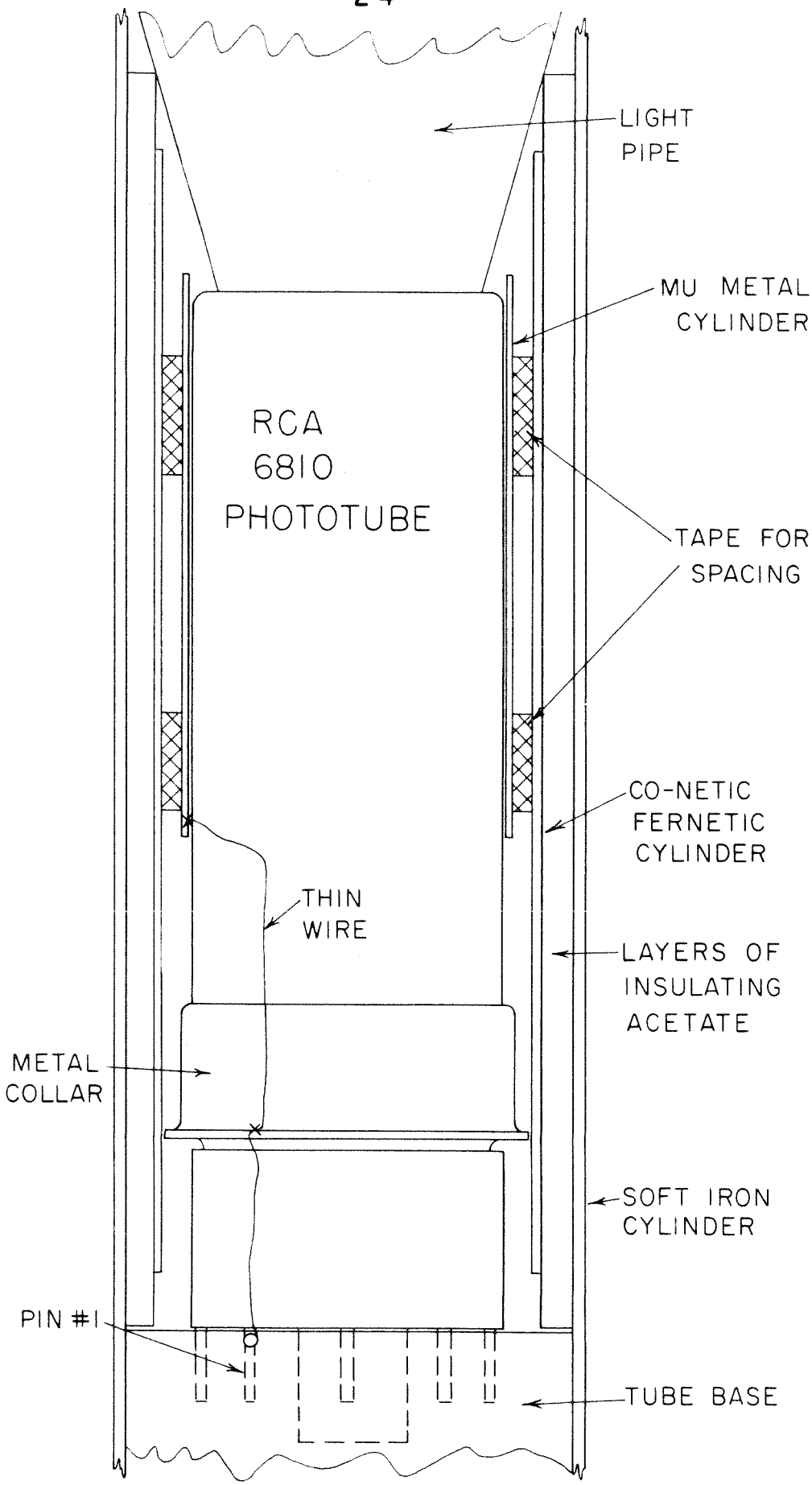
LIGHT PIPE
MU METAL CYLINDER
RCA 6810 PHOTOTUBE
TAPE FOR SPACING
CO-NETIC FERNETIC CYLINDER
THIN WIRE
LAYERS OF INSULATING ACETATE
METAL COLLAR
SOFT IRON CYLINDER
PIN #1
TUBE BASE

The energy loss in the counter is subject to a statistical fluctuation caused by a particles's ability to knock out high energy electrons or delta rays, and this is known as the Landau Effect. The shape of the expected energy loss spectrum has been calculated by Symon (12) and it is shown in figure 17, superimposed on an actual counter's spectrum.

A second factor producing poor counter resolution is the light gathering efficiency from various parts of the counter. This effect has been reduced somewhat by the use of a phototube at each end of the counter, but variations still exist. Another factor pertaining to the light gathering is statistical fluctuations in the light reflected or absorbed and the number of photoelectrons knocked off of the phototube cathode.

In the particular use the counters were being put to, the particles had a range of momenta $\frac{\Delta P}{P} \approx .1$ and consequently some variation in velocity. For the highly relativistic particles this made little difference, but for the others the resolution could be considerably broadened, especially near the end of the particles's range.

In an attempt to improve the pulse height resolution, a counter was built having a scintillator 4 cm. thick and viewed by 5" phototubes. This would tend to reduce the various statistical fluctuations and increase the light gathering efficiency. The counter provided somewhat better resolution than the normal 2 cm. scintillator with 2" tubes, but it was not felt that the slight improvement in resolution was worth

the increased difficulty encountered due to the large size of the counter and the special high voltages needed.

The spectra of pulse heights produced by 500 MEV/C protons for this counter and a normal 2 cm. counter are shown in figure 5. When pions were investigated, the thin counter performed as well as the thick counter.

D. Čerenkov Counter

The Čerenkov counter was a well polished $1\frac{1}{2}$" thick piece of U. V. T. lucite viewed from both ends by R. C. A. type 6810A photo-tubes. For a particle of charge Z and velocity β going through a medium of refractive index n, Marshall (13) gives the following formulas for the number of photons in a frequency range $\Delta \nu$ and their direction relative to the particle velocity.

$$I = 4\pi z^2 \frac{e}{hc^2} \Delta\nu \left(1 - \frac{1}{\beta^2 n^2}\right)$$

$$\cos\theta = \frac{1}{\beta n}$$

A highly relativistic particle ($\beta = .95$) passing through this counter normal to the face, will produce approximately 760 photons in a wave length range that an S-11 photo cathode will respond to. The photons would be emitted at 45° to the direction of the incident particles and at 45° to all the faces of the rectangular shaped counter, if the particle entered normal to the face. Lucite of refractive index

FIGURE 5

PULSE HEIGHT SPECTRA FOR PROTONS OF MOMENTUM,

P_o = 500 MEV/C

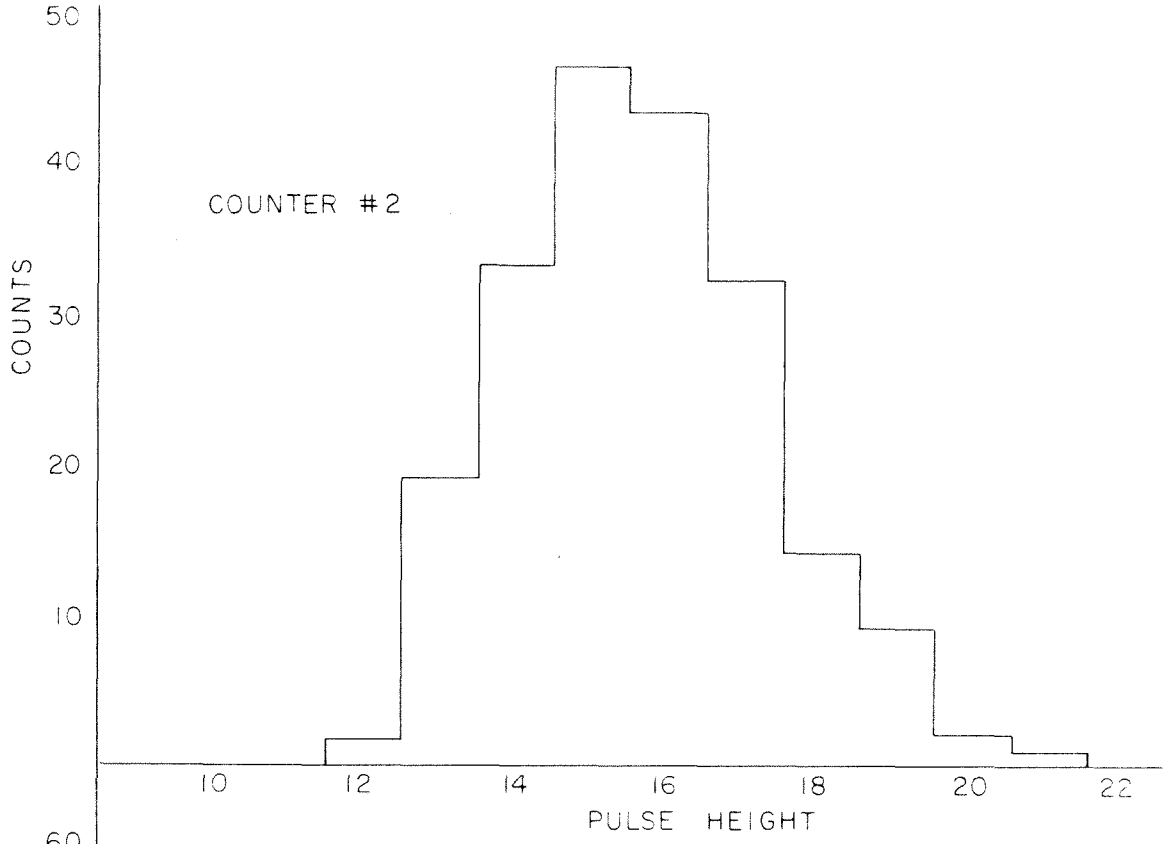
COUNTER #2
COUNTS
50
40
30
20
10
10
12
14
16
18
20
22
PULSE HEIGHT

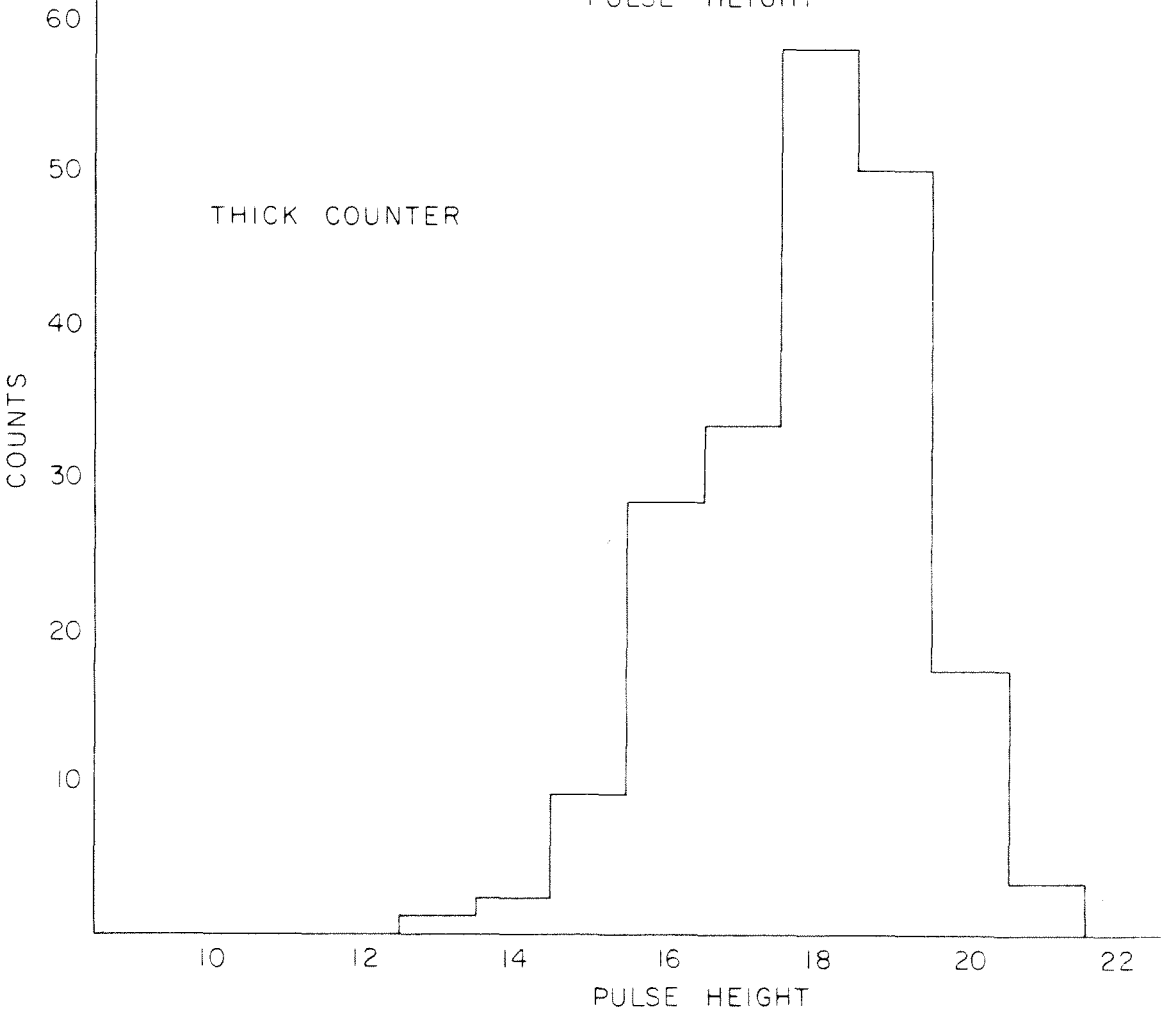
THICK COUNTER
COUNTS
60
50
40
30
20
10
10
12
14
16
18
20
22
PULSE HEIGHT

1.5 has a critical angle for internal reflection of 41.8° and consequently the Čerenkov light will totally reflect off of every face of the counter in optical contact with air and produce a very high light gathering efficiency.

The counter was wrapped in black paper so light that did not totally reflect, but escaped the counter, would not be reflected back into the counter or toward the cathode. This was done in an attempt to reduce the efficiency for particles of $\beta < .9$, since they produce light in a more forward direction which hits the large faces of the counter at angles less than 41°. It was hoped that the black paper would also reduce the efficiency in counting slow particles which might have induced the lucite to scintillate weakly.

The signal from the phototubes was amplified by a Hewlett Packard Model 460A amplifier and then placed in fast (20mμ sec.) coincidence with the signal from a scintillation counter. The efficiency of the Čerenkov counter for a $\beta = .95$ particle was estimated in the following manner.

Photons produced in desired spectral range	760
Light gathering efficiency	26 °/o
Photons striking cathode in desired spectral range	200
Average cathode efficiency over this range	5 °/o
Average number of electrons produced by cathode	10

Using the Poisson formula, $f(x) = \frac{e^{10}\, 10^{x}}{X!}$, to determine the probability of getting x electrons, the efficiency of the counter can be estimated if it is assumed that a signal of n or more electrons

from the cathode will trigger the coincidence circuit.

TABLE IV.

Photo-electrons Produced vs. Efficiency for Čerenkov Counter

n	Efficiency °/o
0	100
1	99.99
2	99.95
3	99.7
4	98.9
5	97
6	93
7	87
8	78
9	66

Assuming an electron amplification of 10^7 for the phototubes, each electron from the cathode will produce a pulse of 10^7 electrons of 3×10^{-9} seconds duration at the anode. The anode capacities were of the order of 10^{-11} farads and the signal cable and terminations (in parallel) were 180 ohms each.

At the output of the HP amplifier of gain 10, the single electron signal would be about .2 volts which was nearly what was required to turn off the tube in the coincidence circuit. This would lead to efficiencies in the high 90 °/o range. The experimentally measured values are shown in figure 6.

FIGURE 6

EFFICIENCY OF ČERENKOV COUNTER FOR DETECTING PARTICLES OF VELOCITY β

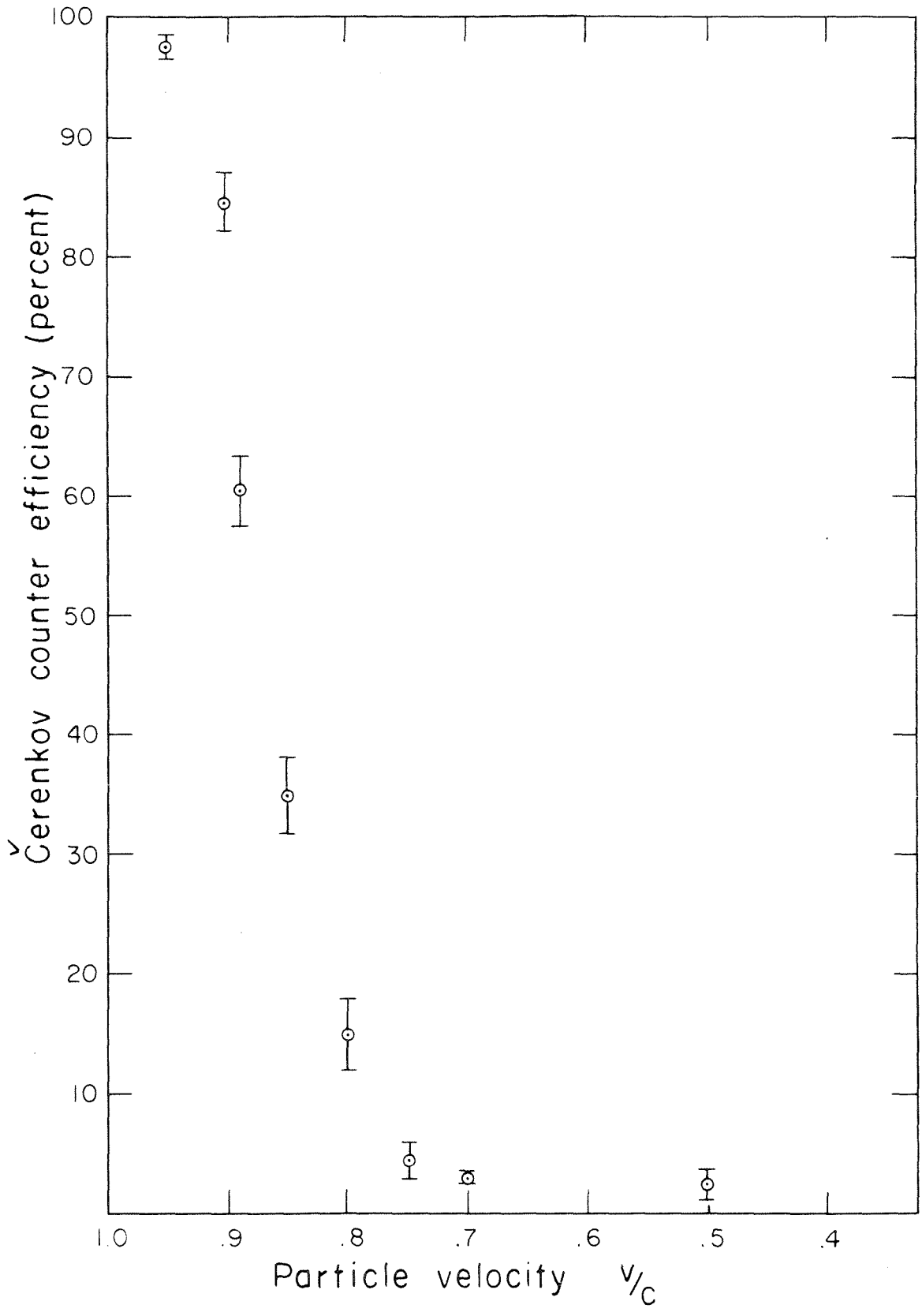
100
90
80
70
60
50
40
30
20
10
Cerenkov counter efficiency (percent)
1.0
.9
.8
.7
.6
.5
.4
Particle velocity v/c

The number of particles of velocity below the Čerenkov threshold that would be detected, can be estimated if it is assumed that the lucite does not scintillate at all. The probability for a particle of zero spin and $\beta = .65$ to knock out an electron of sufficient energy to emit Čerenkov light can be calculated using the formulas given in Rossi's book (14). This calculation shows a 50 °/o probability of this occurring in a 4 cm. lucite counter, but the range of these electrons is in the order of millimeters, whereas the pions normally detected give out light for all 4 centimeters. In order to have a reasonable chance of being detected, the particle would have to knock out very many electrons.

From this analysis, an upper limit of a few per cent can be put on the detection due to these knock on electrons.

The output of the Čerenkov counter was placed in fast coincidence with the output of C-3 in an effort to reduce the possibility of accidental events being caused by noise generated in the phototube. Because of the low light levels encountered in Čerenkov work, high gains were required to obtain the high efficiency desired, and even a single thermal electron emitted from the cathode could produce an appreciable signal. In an attempt to reduce the noise problem further, the phototubes to be used were carefully selected to have a very low noise level, and they were always run at voltage less than 2000 volts. The coincidence circuit used was model 10-T-359 and it was equipped with "infinite" (terminated with the characteristic impedence of the cable) clipping stubs, providing a time resolution determined by the

length of the phototube pulses. Shorter clipping stubs were not used in an effort to insure high efficiency and because the accidental rate did not have to be reduced further. An upper limit on the accidental rate was set by the experimentally determined detection efficiency for protons of a velocity below the Čerenkov threshold.

A series of experimental runs was taken to determine the efficiency of the Čerenkov counter as a function of particle velocity. The particles used were pions, and in some cases there was a slight electron contamination. This did not make any appreciable difference at the higher velocity points, but at the $\beta = .7$ and $.75$ points where the pion counting rate was very low, the results obtained must be taken as an upper limit. One point ($\beta = .5$) was taken with protons as a check to see if weak scintillations were causing particles to be detected, and this does not appear to be the case. The results of these runs appear in figure 6.

F. P. Dixon checked the efficiency for this counter using protons and pions with the high momentum magnet, and the results are in substantial agreement. The efficiency he measured for the $\beta = .7$ protons was approximately 2 $^{o}/_{o}$.

E. Counters Designed to Eliminate Scattered Particles

One of the principal sources of false K-like particles came from protons of momenta other than the momentum for which the magnet was set. These particles could scatter from the pole pieces, lead slits or apertures, and pass through the scintillation counter. Any such

particle having a velocity comparable to the K velocity could produce an event indistinguishable from the real K meson events.

In an attempt to eliminate these scattered particles a counter was designed to fit into the aperture of the magnet. The geometry of this counter was such that any particle emitted from the hydrogen in the target and passing through this counter could not strike the pole tips or the lead slits. The counter was located 61" from the center of the target and was trapazoidal in shape. Its dimensions were as follows:

Thickness	1/4"
Height	12-5/8"
Top Width	5/8"
Bottom Width	1-31/32"

Since the counter defined the aperture of the magnet (and the solid angle), it was possible to remove the lead jaws, which were used to define the vertical aperture and eliminate another possible source of scattering.

Unfortunately, protons emitted from sources other than the hydrogen in the target, such as the target walls and air path, could pass through this counter and scatter into the detectors. When empty target runs were taken, the number of scattered protons counted was the same as the full target counting rate within the statistical accuracy.

A second disadvantage of this system was that it reduced the counting rate by a factor of two, due to the shape and size of this aperture counter.

Because this counter was placed within the magnetic field, the very low momenta particles emitted from the target were swept away before they could reach it. The resultant reduction in counting rate allowed experiments to be conducted at angles as low as 10^{o} in the laboratory, with no absorber required in front of the counter. In a previous experiment (1) at 15^{o}, with a conventional counter outside of the magnetic field, it was necessary to use 3" of carbon absorber. This magnetic sweeping effect was verified by measuring the counting rate in the aperture counter, with and without the magnetic field. At small angles this ratio was the order of 1 to 8. To insure that this was not due to the effect of magnetic field on the phototube, a cobalt source was measured with and without the field, and the pulse heights showed no change at the field strengths used.

The equipment was revised in an attempt to eliminate scattered particles from all sources, increase the counting rate and still retain the advantages of a front counter located in the aperture of the magnet.

R. L. Walker suggested a system where a series of thin counters would be installed along the magnet pole pieces in such a manner that any particles scattering from the iron would produce a signal in the counters.

An arrangement of four scintillating strips on each pole face, designed by A. M. Wetherell and built by J. Boyden, was installed in the magnet and proved successful in eliminating most of the scattered particles. The four strips were individually joined to light pipes and

the other end of the four light pipes placed in optical contact with the face of a 6810 photomultiplier tube. Because the strips appear to fan out from the phototube, they were called "fan counters" and will be referred to as such hereafter. The four strips were positioned (figure 7 and 8) in such a manner that no particle produced in the hydrogen could scatter off the pole face into the rear counters and not pass through a strip. However, there was still a very slight chance for a particle produced elsewhere to scatter into the detectors and consequently some scattered particles appeared in the K runs.

One of the problems concerning the fans involved the phototubes working in the high magnetic fields near the coils. Figure 9 shows the magnetic shielding used in an attempt to minimize the change in gains due to the field. At full magnetic field the pulse heights were reduced by no more than 20 $^{o}/o$ of their no field value.

A second problem was the light absorption in a long length of the scintillator. By using a cobalt source, the relative pulse heights from points A and B in figure 8 were measured and found to be of the order of 2 to 1. This meant that only 50 $^{o}/o$ of the light was being lost in transmission, a figure well within the acceptable range.

The pulse height with the source at point B was compared to the pulse height obtained by placing a piece of the same scintillator in optical contact with the phototube. This ratio came out 1 to 10, and at present there is no satisfactory explanation of this apparently large loss of light. However, there was still sufficient light transmitted to allow the phototubes to run in their normal voltage range (1900 volts)

FIGURE 7

POSITION OF FAN COUNTERS (SIDE VIEW)

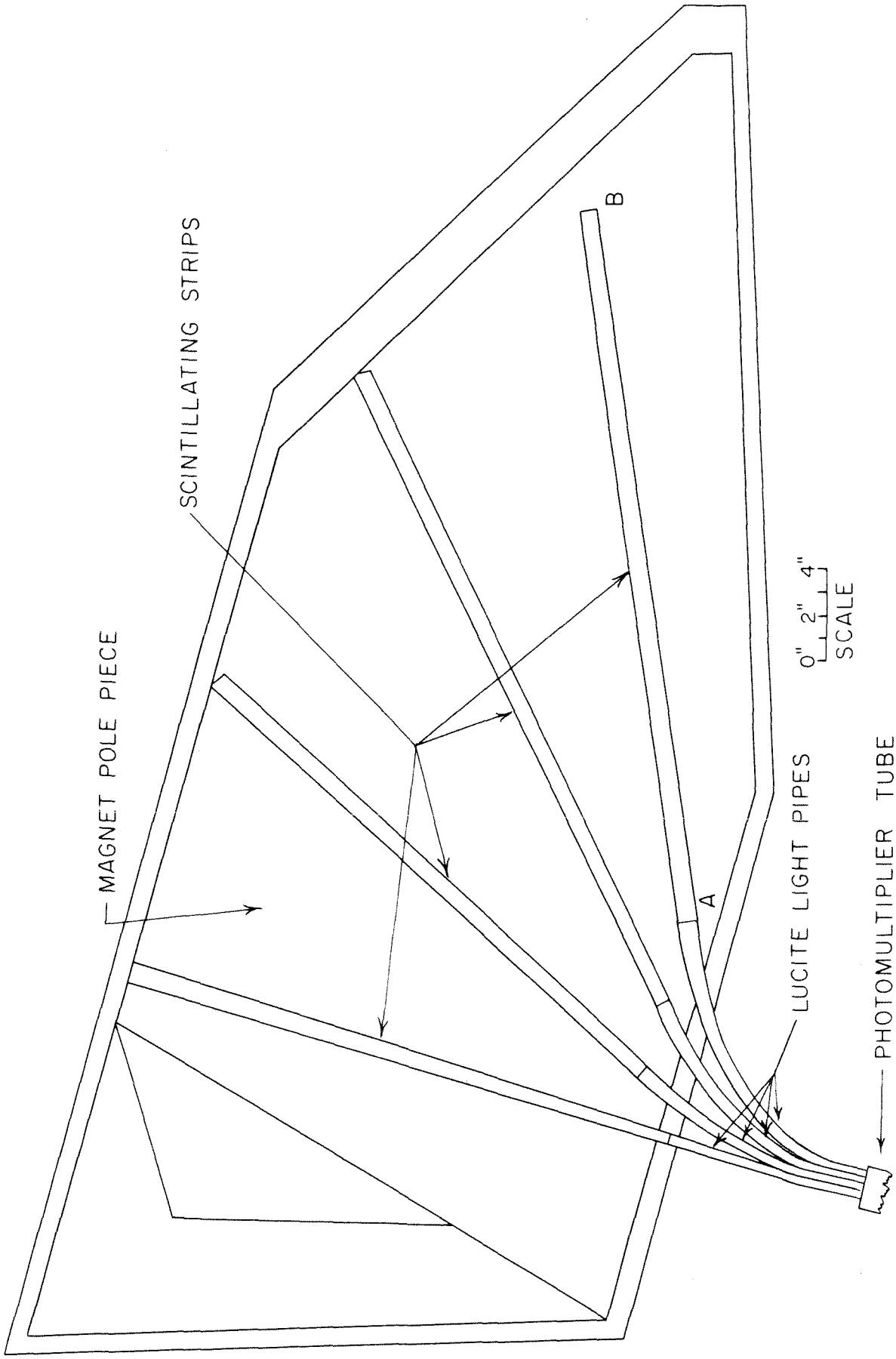
MAGNET POLE PIECE
SCINTILLATING STRIPS
B
A
0" 2" 4"
SCALE
LUCITE LIGHT PIPES
PHOTOMULTIPLIER TUBE

FIGURE 8

POSITION OF FAN COUNTERS (TOP VIEW)

The rays indicated in the figure are the limiting trajectories for particles emitted from the hydrogen and the outer target walls. Fringe field focussing has been neglected.

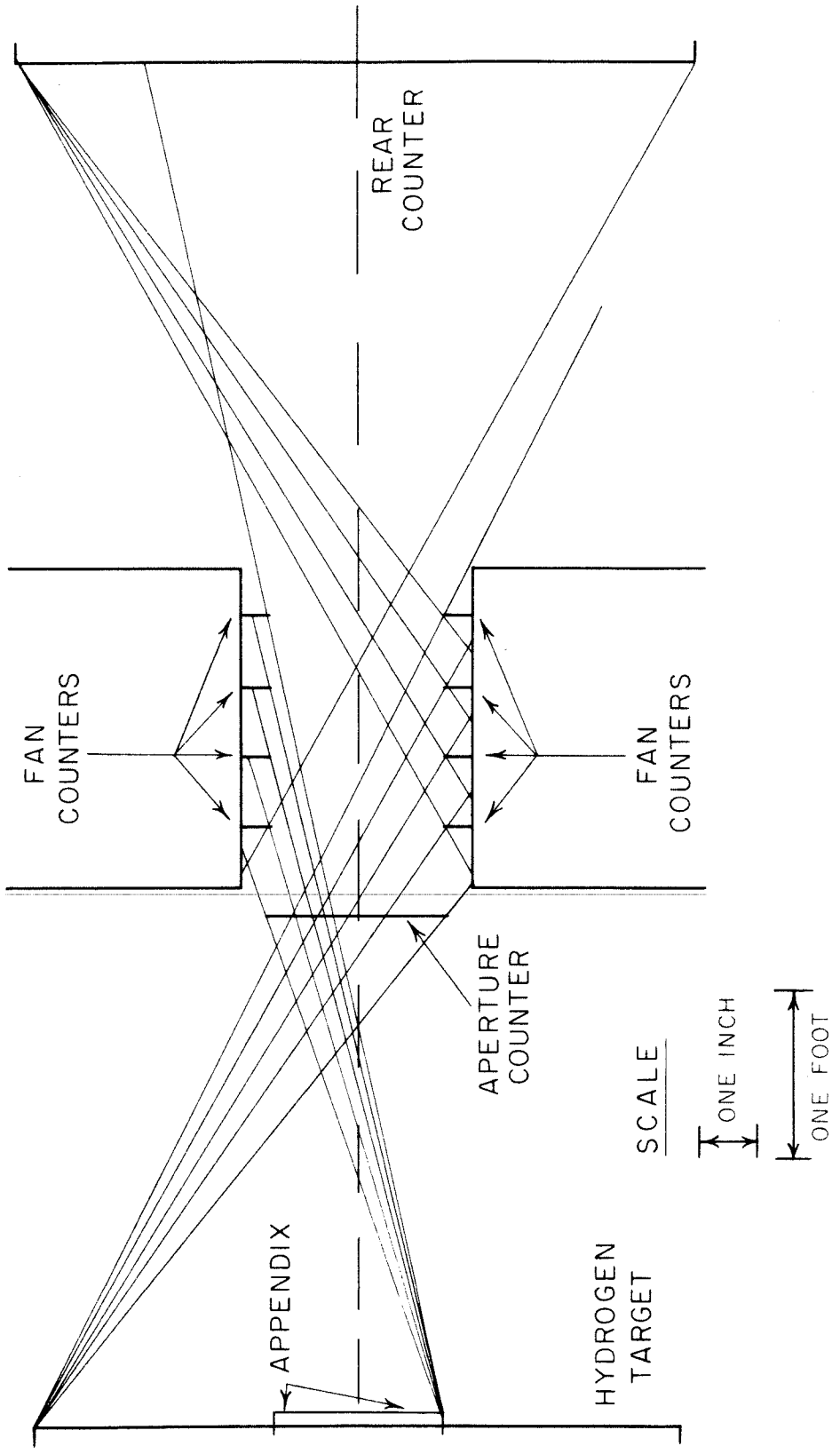
REAR COUNTER
FAN COUNTERS
FAN COUNTERS
APERTURE COUNTER
APPENDIX
HYDROGEN TARGET
SCALE
ONE INCH
ONE FOOT

FIGURE 9

MAGNETIC SHIELDING OF FAN PHOTOTUBES

The shielding within the soft iron cylinder is very similar to that shown in figure 4 and consequently has not been reproduced here in detail. Additional "caps" of Fernetic foil and mu metal were added as shown in an attempt to prevent the flux from penetrating the phototube.

The two layers of thick soft iron shielding enclosed both tubes and the light pipes emerged through square holes.

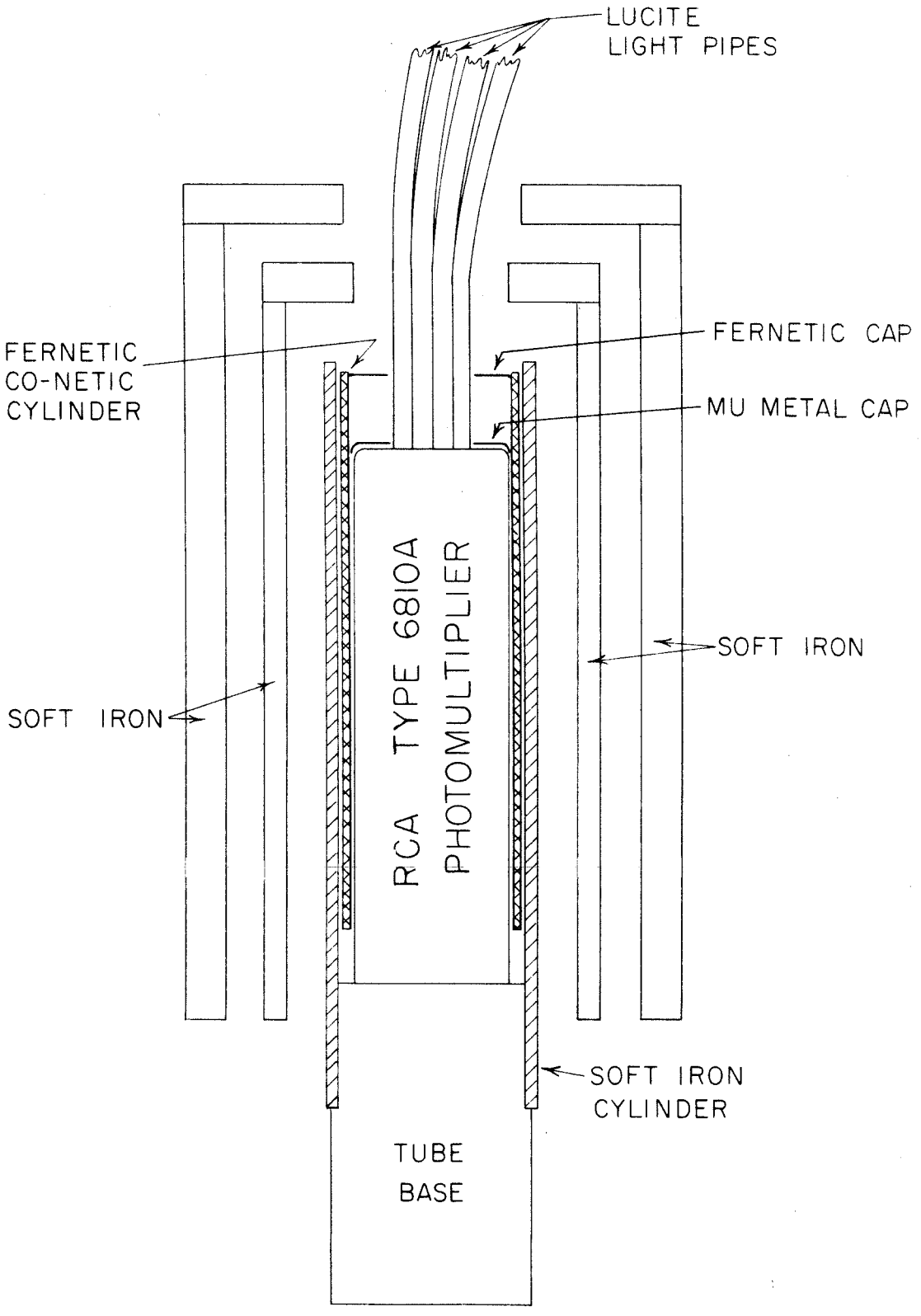
LUCITE
LIGHT PIPES
FERNETIC
CO-NETIC
CYLINDER
FERNETIC CAP
MU METAL CAP
RCA TYPE 6810A
PHOTOMULTIPLIER
SOFT IRON
SOFT IRON
SOFT IRON
CYLINDER
TUBE
BASE

and provide a large enough output signal to drive the coincidence circuit.

The two sets of fan counters were viewed by 6810 phototubes and their signals added at a coincidence circuit (10-T-359). The signal used in coincidence was from the 6810 phototube on the last counter. A fast coincidence circuit was needed to eliminate accidentals, due to the high counting rates in the fans, especially at far forward angles. The lower limit of resolving time that could be used in this circuit and still retain a high efficiency was determined by geometrical considerations. There was a spread of many mμ seconds in the timing due to the position where the fan was struck and the subsequent particle trajectory. To provide as uniform an output pulse as possible under these circumstances, one of the clipping stubs was "infinite" and one was clipped fairly short. The photographs of the output pulse showed very few small pulses, which was an indication that this technique seemed to work well. The fact that the fraction of events vetoed on the pion runs agreed well with the geometrical prediction was an indication of the high efficiency obtained.

From the observed counting rates, the fan veto circuit was estimated to veto approximately 3/4 $^{o}/_{o}$ of the real events due to accidental coincidences.

In the place of the narrow aperture counter, a scintillator, 3"x12-5/8", was placed in the aperture of the magnet and this counter defined the vertical aperture while the rear fan counters defined the horizontal aperture.

During both π calibration runs and K runs, the output of the fan coincidence circuit was displayed on a scope along with other pulses and the trace photographed. From these pictures it was possible to determine the nature of the particles being vetoed and obtain other useful information. The veto pulses appeared on 20 $^{o}/o$ of the scope traces obtained from π runs and these events were in every way indistinguishable from the events with no veto pulse. It was calculated that the fan counters would reduce the solid angle by an amount somewhat under 20 $^{o}/o$, and the small difference could be attributed to scattered particles.

On the K runs, the veto pulse appeared on 40 $^{o}/o$ of the traces photographed. Since 20 $^{o}/o$ was an upper limit on the vetoing due to pure geometrical considerations, it had to be concluded that at least 20 $^{o}/o$ of the events observed were scattered particles.

The pulse height spectra of these vetoed events are included as figure 16 for comparison with the pulse heights for a normal K run.

F. Time of Flight Circuit

The electronic circuitry and related equipment used in measuring the time of flight between a counter located in the aperture of the magnet and a counter in the rear (a distance of $2\frac{1}{2}$ meters) had to have extremely fast time response to distinguish between π snd K mesons. At the momentum used for obtaining most of the data, 425 MEV/C, the difference in time of flight had an average value of 4 mμ sec. However, the actual time of flight for a particle could vary by a few mμ seconds, because of the $\frac{\Delta P}{P}$ momentum acceptance of the magnet,

and the variation in lengths of the possible flight paths. For the π, this difference in flight path amounted to about 1 $m\mu$ sec., while the variation in velocity with momenta was negligible. For the K mesons, these effects contributed about 2 and 1 $m\mu$ sec. respectively.

The aperture counter, being over 12" long, tended to compensate for some of this variation. Particles with a long flight path would pass through the top of the counter and the light signal would require an extra $1\frac{1}{2}$ $m\mu$ sec. to reach the phototube as compared to light produced by particles passing through the bottom of the counter and having a short path length. On the other counter used as the other input to the time of flight circuit, the effects of light transit times were reduced to a fraction of a $m\mu$ sec. by viewing the scintillator at both ends with phototubes and adding the signals. Extensive tests were conducted on this counter with the coincidence circuit to determine the correct delay to employ between the tubes and the variations of delay with the voltage applied to the phototubes. A result of the series of these tests is shown in figure 10. Even though these delay curves are many $m\mu$ sec. in width, the center can be determined to a fraction of a $m\mu$ sec.

The fast coincidence circuit used was similar to the one used by Donoho and Walker and was based on a design of Wenzel (15) at the University of California Radiation Laboratory. In an attempt to eliminate impedance mismatches, and reduce capacities, the cables leading into the chassis were soldered directly into the circuit, while their other ends were soldered to the phototube bases.

FIGURE 10

DELAY CURVES OF THE TWO PHOTOTUBES

ON C-2 IN COINCIDENCE

These three curves represent 3 delay curves run with one tube at 1900 volts and the other at 1900, 2000, and 2100 volts. They illustrate the variation in transit time with voltage for the electrons in an R. C. A. 6810 phototube.

A cobalt 60 source was used to obtain the data.

One meter of RG 63/U cable corresponds to approximately 4m μ sec.

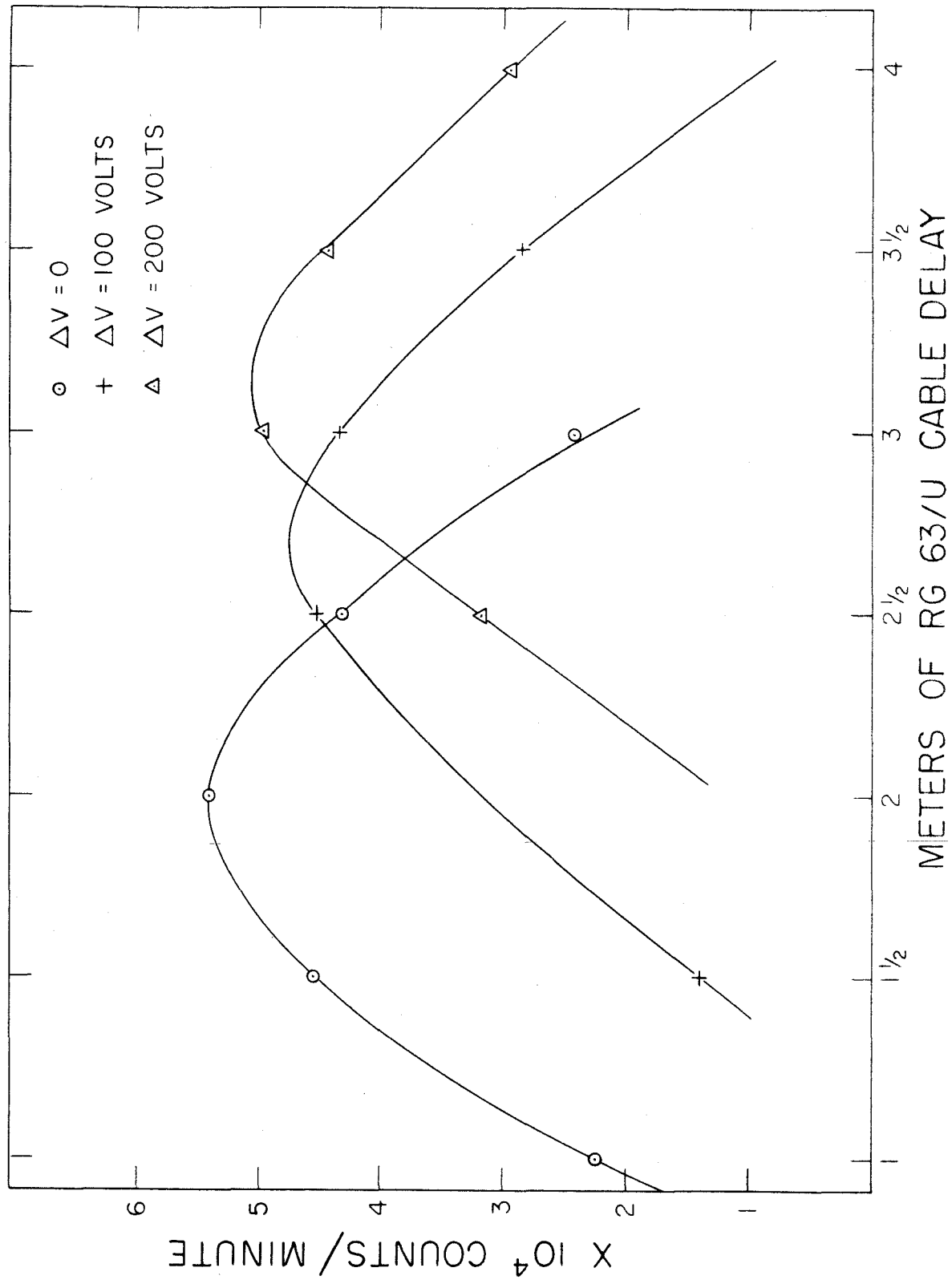
o ΔV = 0
+ ΔV = 100 VOLTS
Δ ΔV = 200 VOLTS
X 10⁴ COUNTS/MINUTE
1
2
3
4
5
6
1½
2
2½
3
3½
4
METERS OF RG 63/U CABLE DELAY

The signal from the aperture counter was delayed by a length of RG 63/U cable added to the existing cable. This delay was changed when various types of particles were investigated and as the momentum setting of the magnet was changed.

The output signal from this circuit was amplified and displayed on a scope in addition to being used in the six channel slow coincidence circuit. The bias of this slow circuit was set very low in an attempt to insure very high efficiency in the electronics and to allow pulse height discrimination to be done at a later time.

The technique of setting a low bias and photographing the time of flight pulse proved very valuable when the gains and biases drifted from day to day, since all the pertinent information was retained on film.

For each K run, the corresponding pion runs were analyzed and the pulse height at which the time of flight was 85 $^{o}/o$ efficient was determined. This value was then used as the criterion for that particular K run. The value of about 85 $^{o}/o$ was chosen to minimize the loss of K mesons and to optimize the pion rejection, which was of the order of 10 to 1.

In the second series of runs there was a small steady drift from day to day in the output of the time of flight circuit. Since each run was individually calibrated, this drift was quite apparent and easily compensated for, as will be explained subsequently.

G. Calibrations

In order to establish this 85 °/o efficiency criterion and to determine experimentally the solid angle and other corrections, several special calibration runs were taken.

The solid angle of the first experimental configuration (narrow aperture counter) was determined by using pions and measuring the ratio of counting rates between this configuration and a "standard" configuration described by Donoho in the magnet report (11). This ratio was $.52 \pm .01$ compared to the geometrical value of .55 . This discrepancy was due in some part to scattering in the aperture counter, inefficiency in the circuit, reduction of $\frac{\Delta P}{P}$ due to energy loss in the counter, and the possibility of a slightly higher counting rate in the "standard" configuration due to slit penetration and scattering.

These data were taken with pions of an energy such that their $P\beta$ product was approximately equal to the $P\beta$ used for the K runs. In this way, the measured results inherently contained the correction for multiple scattering in the aperture counter.

The overall efficiency of the time of flight circuit had to be determined, for even though the biases were set very low, there was still a small probability that an event would be missed completely, and this number must be known. In the first experimental configuration, thick lead slabs were placed in front of the narrow aperture counter in such a manner that they defined an aperture somewhat smaller than the counter. Using protons the counting rate was then simultaneously observed with and without the time of flight circuit required

in coincidence; the ratio of counting rates being the efficiency. This number was determined to be . 99, in good agreement with what was predicted by observing the output pulse height spectra of the circuit.

The entire aperture counter was then removed and the counting rate for protons of momentum P_o = 450 MEV/C increased by $7\frac{1}{2} \pm 1$ °/o. This was the amount expected due to the reduction of the effective $\frac{\Delta P}{P_o}$ of the magnet because of energy loss in the counter. The effects of scattering were estimated to be small and this measurement seemed to confirm this.

During the first series of K runs the spectra of the time of flight output pulses remained the same on every calibration run, within the expected statistical fluctuations. It was then possible to add them all together to determine the pulse height criterion to be chosen. It was also felt that the one measurement of the overall efficiency of the system was sufficient since the pulse height spectra indicated the efficiency to be constant.

In the second experimental configuration the efficiency of the time of flight circuit was measured by placing a smaller counter in front of the aperture counter in such a manner that any particle passing through this small counter and the rear counters had to pass through the aperture counter. The output of this smaller counter was placed in fast coincidence with the third counter in the rear and this coincidence output in slow coincidence with the Čerenkov and middle counters. The efficiency to be measured was then the ratio of counting rates with and without the time of flight in coincidence. Since the time of flight spectra

showed a steady drift in pulse heights from day to day, measurements of the overall efficiency were made several times. The measured efficiencies decreased from 99 °/o to 90 °/o during the course of the experiment in a manner similar to the drift observed in the corresponding pulse height spectra. By examining the correlation between these measurements and the spectra, it was possible to predict very accurately the efficiency of any other run. In the course of the experiment the pulse height at which the time of flight measurement was 85 °/o efficient fell from 28 volts to 15 volts.

F. P. Dixon determined the solid angle of this configuration in a manner similar to that previously discussed. He determined the ratio of pions counted for this configuration and the "standard" configuration described by Donoho in the magnet report (11).

To obtain further information about the actual response of the time of flight circuit, a series of pion runs was made with various time of flight delays and the results are shown in figure 11. The plots have been normalized to represent the same number of pions passing through the system.

A series of K meson runs was taken in an attempt to see if the grouping of K-like particles was due to the setting of the time of flight circuit to a given value. This setting required a particular velocity and therefore might cause a grouping by favoring particles of that velocity out of a random distribution of velocities from spurious particles. The time of flight was set to be 2 mμ sec. longer than K mesons flight time, which would have reduced the velocity in a

FIGURE 11

TIME OF FLIGHT PULSE HEIGHT SPECTRA

FOR VARIOUS DELAYS

The spectrum of pulses produced by pions in the time of flight circuit was obtained in the same manner that calibration runs were obtained.

The bottom spectrum had the signal from the aperture counter delayed by the correct amount (8.5 mμ sec.) for pions. The other spectra correspond to an additional delay of 2, 3, 4 and 5 mμ sec. respectively.

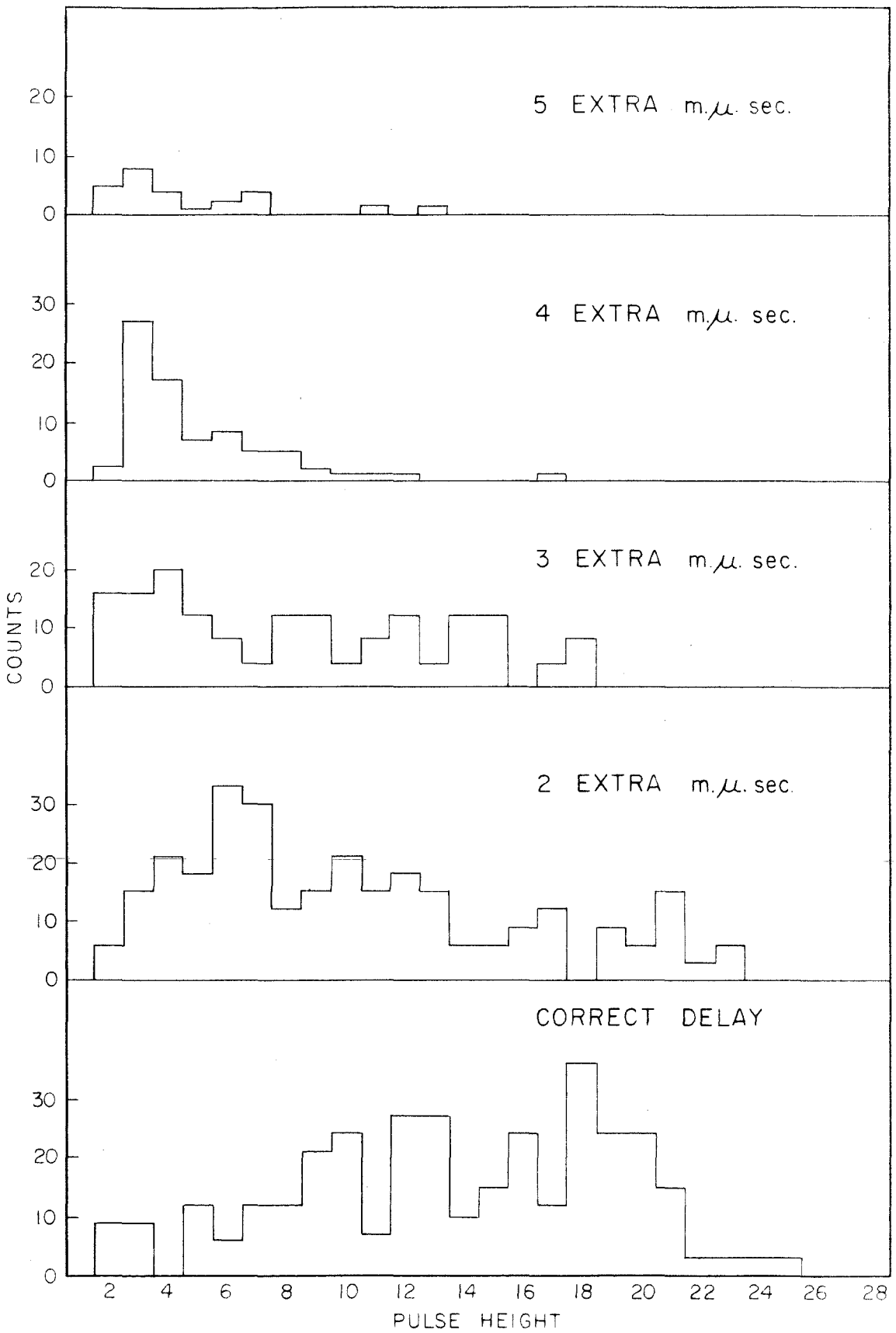
5 EXTRA m.μ. sec.
4 EXTRA m.μ. sec.
3 EXTRA m.μ. sec.
2 EXTRA m.μ. sec.
CORRECT DELAY
COUNTS
PULSE HEIGHT
0
10
20
30
2
4
6
8
10
12
14
16
18
20
22
24
26
28

manner such that the energy loss in the counters would be 25 $^{o}/_{o}$ higher.

Analysis of these pseudo K runs showed no shift in the position of the "K" grouping with about 10 points in the group, and a considerable reduction in the number of π mesons counted. No attempt was made to determine the K detection efficiency under these conditions.

IV. EXPERIMENTAL DATA

A. K Identification

The photographed scope traces were viewed on a 35 mm. slide projector and the height of every pulse was recorded. A number of typical traces are shown in figure 12.

The pion runs were analyzed by plotting histograms of the pulse height in the individual counters and the time of flight circuit. Because the three scintillation counters and their associated electronics did not seem to be subject to drift in gain, the pulse height spectra from all the runs with a given configuration were added to form a master graph for each counter. This same method was used for the time of flight analysis during the first set of runs, but for the second set, they were individually analyzed and an 85 $^{o}/o$ limit set for each run. From the known energy loss for K and π mesons at a given momentum, and because of the linearity of the electronics, it was possible to predict the limits of the expected K meson pulse heights.

The K runs were analyzed in the following manner. All events containing a time of flight pulse below the minimum value set by the calibration runs, or a fan counter veto pulse, were discarded. The remaining events were analyzed by making a "dot plot" of the pulse heights on single cycle log paper. On a "dot plot" every event was represented by a dot whose coordinates are the value of the pulse height in C-1 (first counter) and C-2 (second counter). The dot was plotted in a color (which does not show here) in order to indicate whether the pulse height in C-3 (third counter) was or was not within the limits

FIGURE 12

TYPICAL OSCILLOSCOPE TRACES

The first three pulses are outputs of the three scintillation counters. The fourth pulse is the fan veto circuit and the last pulse is produced by the time of flight circuit.

Trace A is a pion on a calibration run. Trace B is an event identified as a pion on a K run because the pulse heights indicate a minimum ionizing particle and a time of flight different from the K time of flight.

Trace C was caused by a K meson and Trace D is a vetoed event on a K run.

A

B

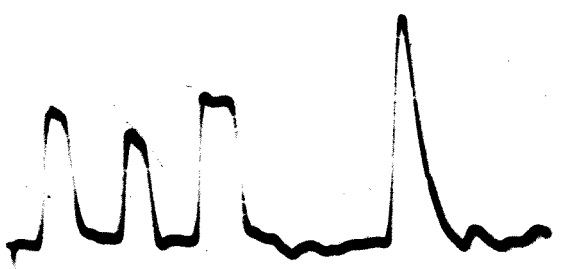

C

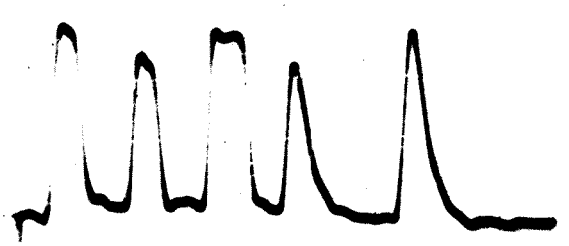

D

predicted for K mesons.

The limits of the predicted pulse heights for K mesons in the other two counters were indicated by dashed lines on the dot plots. Within these predicted limits there was a good bunching or grouping of points which were tentatively identified as K mesons. Only rarely did an event falling within these limits have a pulse height outside of the limits set for C-3. Only a small fraction of the events that were outside of the limits for C-1 or C-2 fell within the C-3 limits. The events that were minimum ionizing in C-1 and C-2, but larger in C-3 could easily be explained by the interaction of pions or electrons in the $\frac{1}{2}$" piece of lead placed between C-2 and C-3.

The dot plots for the 514 MEV/C and two of the 420 MEV/C points are shown in figures 13-16, and in addition two empty target runs are shown. Figure 15a is an empty target run taken with the first experimental configuration and the scattered protons are in evidence. Figure 15b, an empty target run taken using the fan counters, shows a great deal less in the way of scattered protons. Figure 16b is a plot of the events with the correct time of flight but containing a fan veto pulse. These data were taken at the same time as the data in figure 16a. From the analysis done earlier, it was concluded that at least half of these events were actually caused by particles scattered from the pole faces. This figure shows clearly the advantage gained from the fan counters.

To check the consistency of the K identification analysis, the single pulse height spectra in all three counters were plotted for the

FIGURE 13

PULSE HEIGHT CORRELATION (DOT PLOT)

Θ lab = 10^{o}

E_{o} = 1070

P_{o} = 514 MEV/C

7911 bips

Figure 13a shows all events with correct pulse height from time of flight circuit.

Figure 13b shows only those events in figure 13a which had a pulse height in C-3 within the K limits.

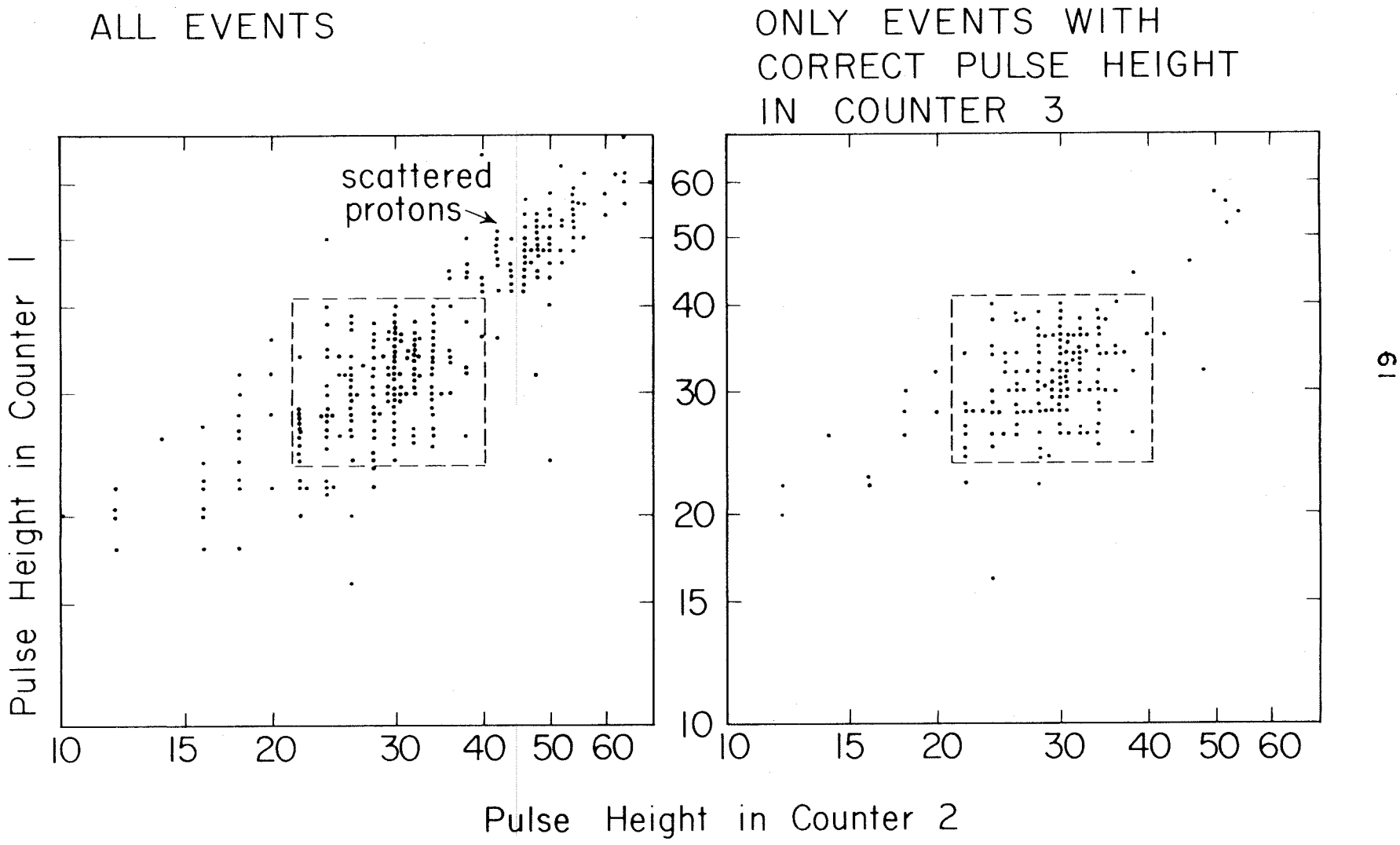
ALL EVENTS
ONLY EVENTS WITH CORRECT PULSE HEIGHT IN COUNTER 3
scattered protons
Pulse Height in Counter 1
Pulse Height in Counter 2
10
15
20
30
40
50
60

FIGURE 14

PULSE HEIGHT CORRELATION (DOT PLOT)

$P_o = 420$

$\theta lab = 25^o$

$k = 1000$ MEV

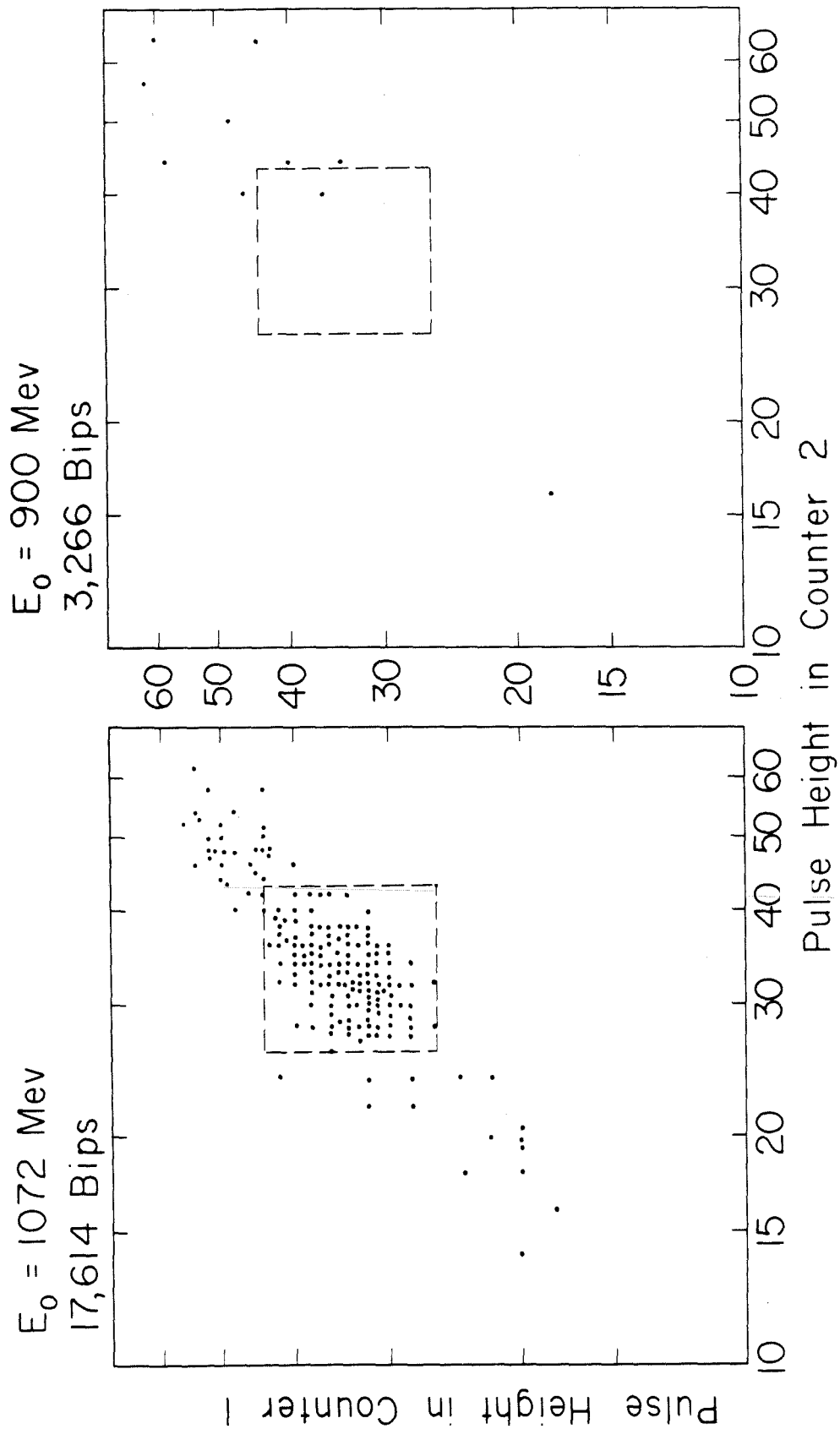
E_0 = 1072 Mev
17,614 Bips
E_0 = 900 Mev
3,266 Bips
Pulse Height in Counter 1
Pulse Height in Counter 2
10
15
20
30
40
50
60

FIGURE 15

PULSE HEIGHT CORRELATION (DOT PLOT)

Empty target runs at 10^{o} lab with the narrow aperture counter (P_o = 514 MEV/C, 4729 bips) and with the fan counters (P_o = 422 MEV/C 3000 bips).

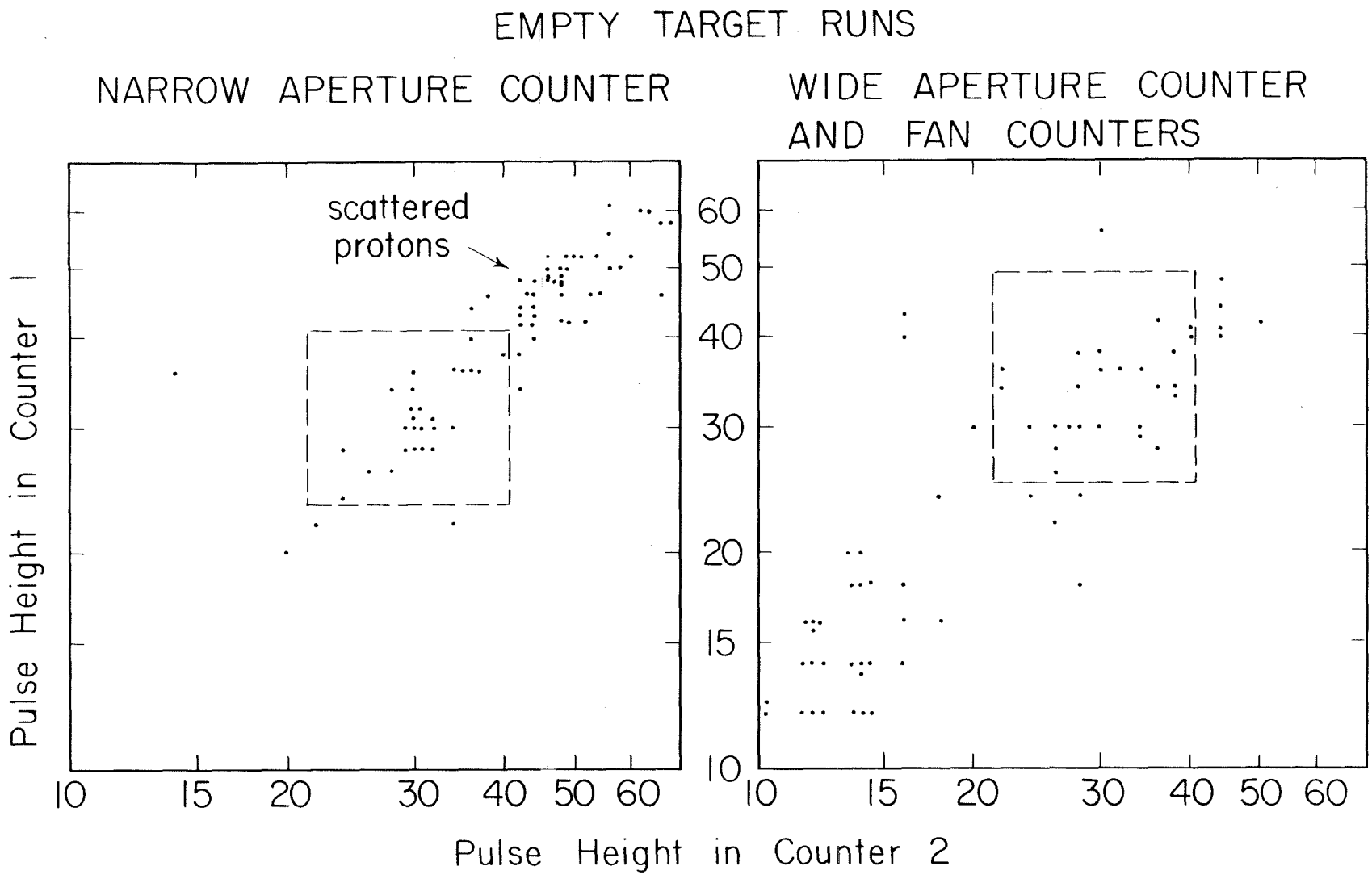
EMPTY TARGET RUNS
NARROW APERTURE COUNTER
WIDE APERTURE COUNTER
AND FAN COUNTERS
scattered
protons
Pulse Height in Counter 1
Pulse Height in Counter 2
10
15
20
30
40
50
60

FIGURE 16

PULSE HEIGHT CORRELATION (DOT PLOT)

P_o = 422 MEV/C

θ lab = 25^o

15, 000 bips

These data were taken simultaneously. The events with a veto pulse are in figure 16b; without in figure 16a.

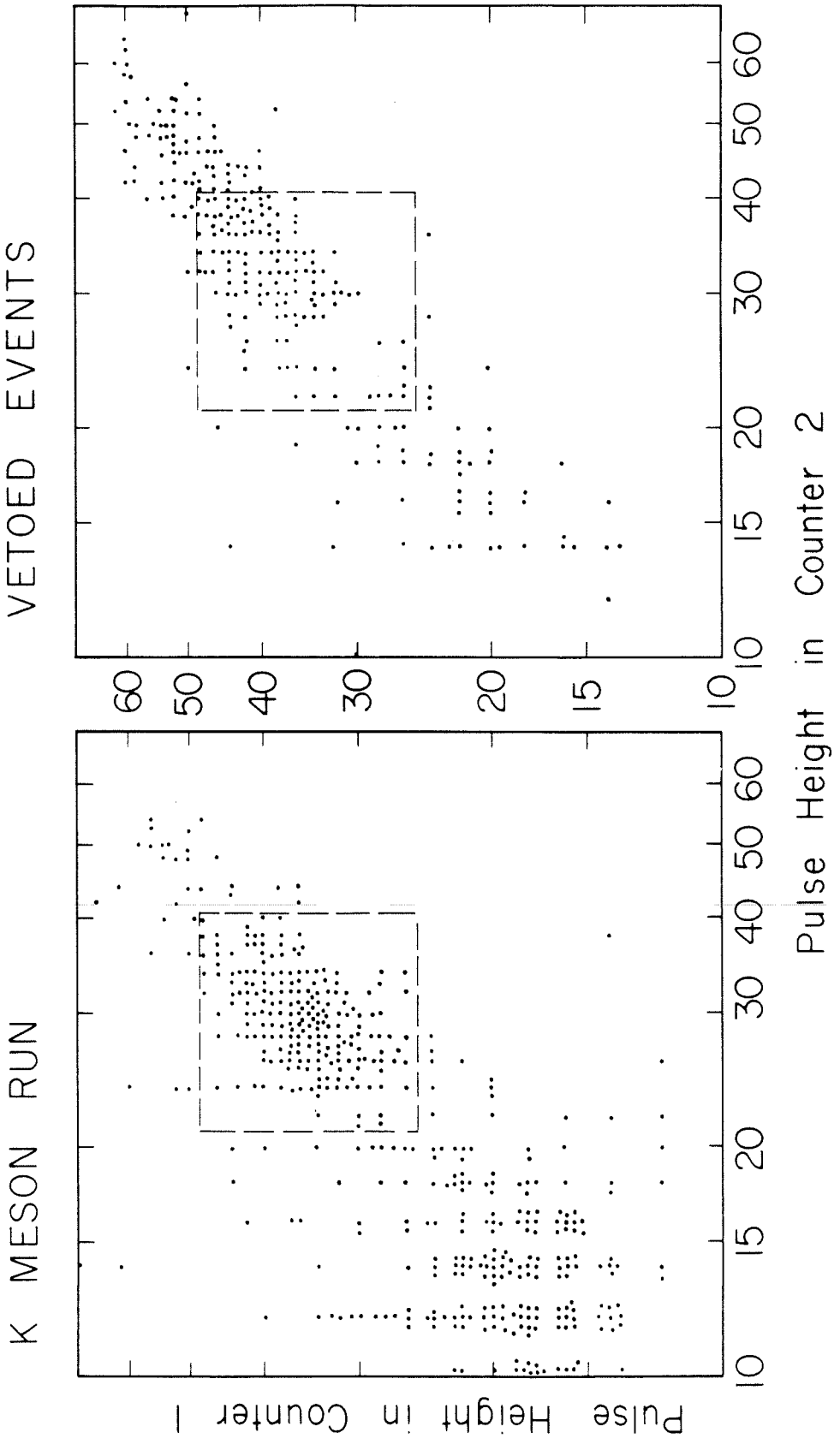
K MESON RUN
VETOED EVENTS
Pulse Height in Counter 1
Pulse Height in Counter 2
10
15
20
30
40
50
60

K runs. These were divided into groups which were and were not considered K's from the analysis of the other two counters. These plots, shown in figures 17-20 are for the 10^{o}, 514 MEV/C point and the first 25^{o}, 420 MEV/C point. In addition C-3 is shown for part of the second 25^{o} run. When these data were compared to the corresponding pion data the K mesons seemed to fall exactly where predicted with about the expected counter resolution.

In the second 25^{o} run, shown in figure 20, the Čerenkov counter was not working as efficiently as in the other runs and another peak was visible, whereas, in the other data (figures 17-19) there was only a trace of it. These pulses, attributed to pions, produced a spectrum very much like the spectra obtained when pion runs were taken. Many of the larger events were particles that might have done something "abnormal" such as decaying in flight, producing a star, or scattering from some unlikely place because by requiring no Čerenkov signal and a long time of flight a very strong bias was placed in favor of "unusual" events relative to normal pion counts.

In the course of accumulating the data shown in figure 20, approximately 0.25×10^{6} pions went through the system and less than two per thousand were counted. When the Čerenkov counter was working well, the number of pions was reduced by a factor of about 5 as is shown in figures 17-19.

The events with large pulse heights in all three counters came from scattered protons which have not been eliminated by the measures

FIGURE 17

SINGLE COUNTER SPECTRA

The spectrum of pulse heights from the calibration runs and the spectrum of pulse heights from the K runs are shown for C-1 with P_o = 420 MEV/C. The events that are indicated by cross hatching are those that are identified as K mesons by their pulse heights in C-2 and C-3 alone.

The dotted curve on the pion spectrum is the expected shape due to the Landau Effect only.

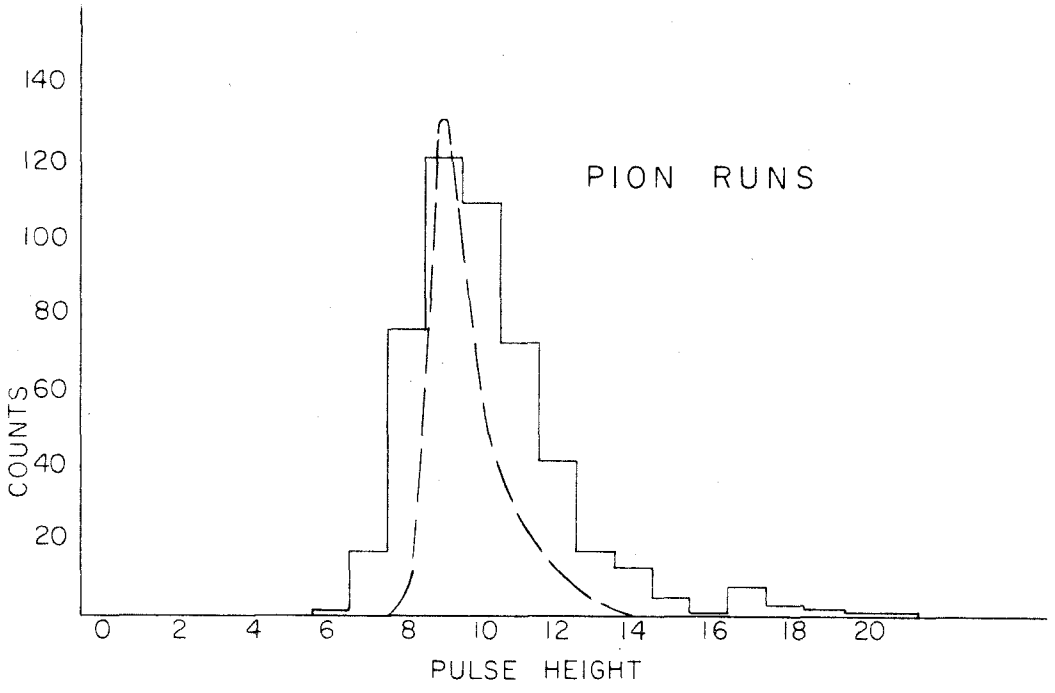
PION RUNS
COUNTS
140
120
100
80
60
40
20
0
2
4
6
8
10
12
14
16
18
20
PULSE HEIGHT

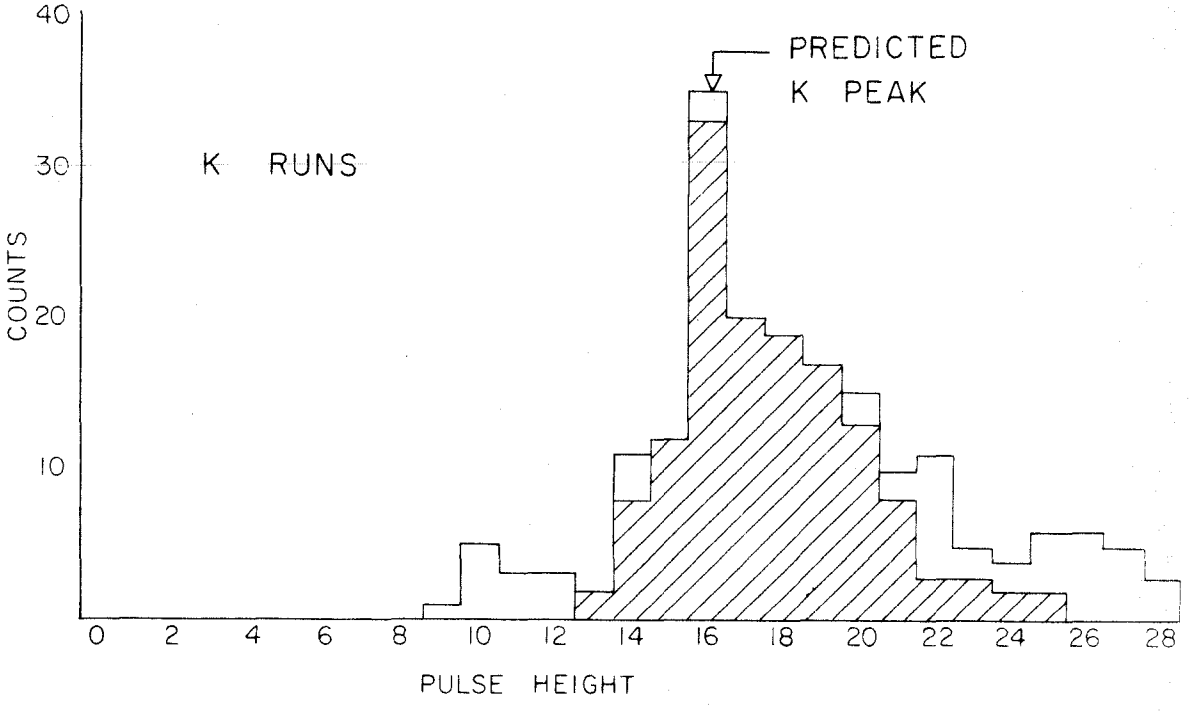
PREDICTED
K PEAK
K RUNS
COUNTS
40
30
20
10
0
2
4
6
8
10
12
14
16
18
20
22
24
26
28
PULSE HEIGHT

FIGURE 18

SINGLE COUNTER SPECTRA

The spectrum of pulse heights from the calibration runs and the spectrum of pulse heights from the K runs are shown for C-3 with P_o = 420 MEV/C. The events that are indicated by cross hatching are those that are identified as K mesons by their pulse heights in C-1 and C-2.

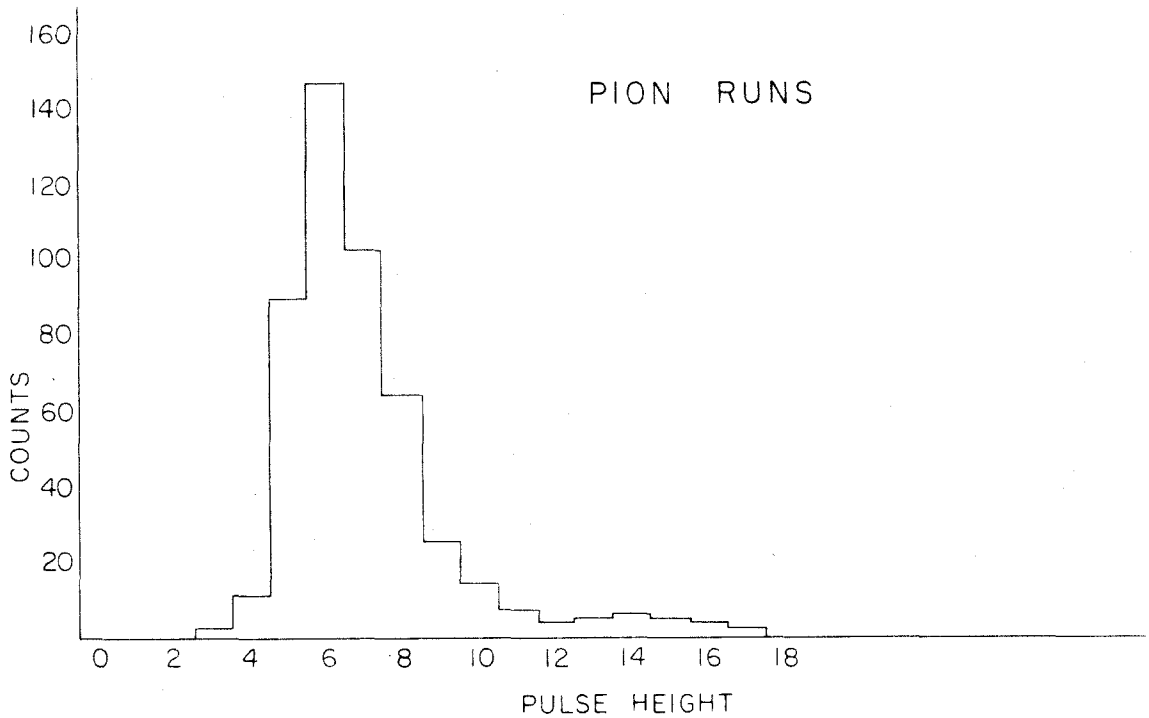
PION RUNS
COUNTS
160
140
120
100
80
60
40
20
0
2
4
6
8
10
12
14
16
18
PULSE HEIGHT

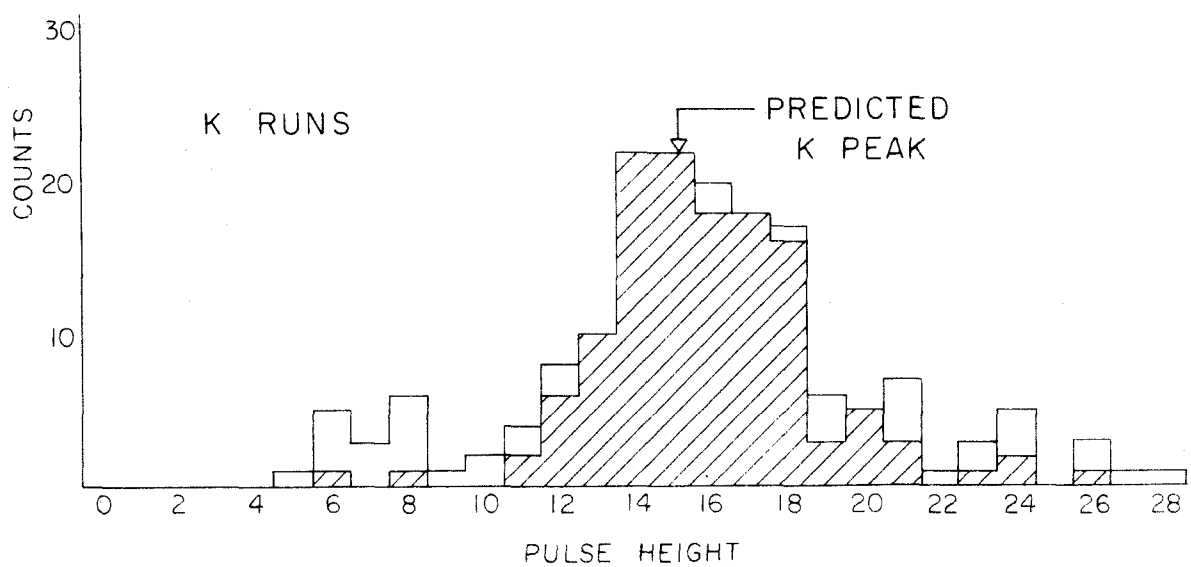
K RUNS
PREDICTED
K PEAK
COUNTS
30
20
10
0
2
4
6
8
10
12
14
16
18
20
22
24
26
28
PULSE HEIGHT

FIGURE 19

SINGLE COUNTER SPECTRA

The spectrum of pulse heights from the calibration runs and the spectrum of pulse heights from the K runs are shown for C-3 with P_o = 514 MEV/C. The events that are indicated by cross hatching are those that are identified as K mesons by their pulse heights in C-1 and C-2.

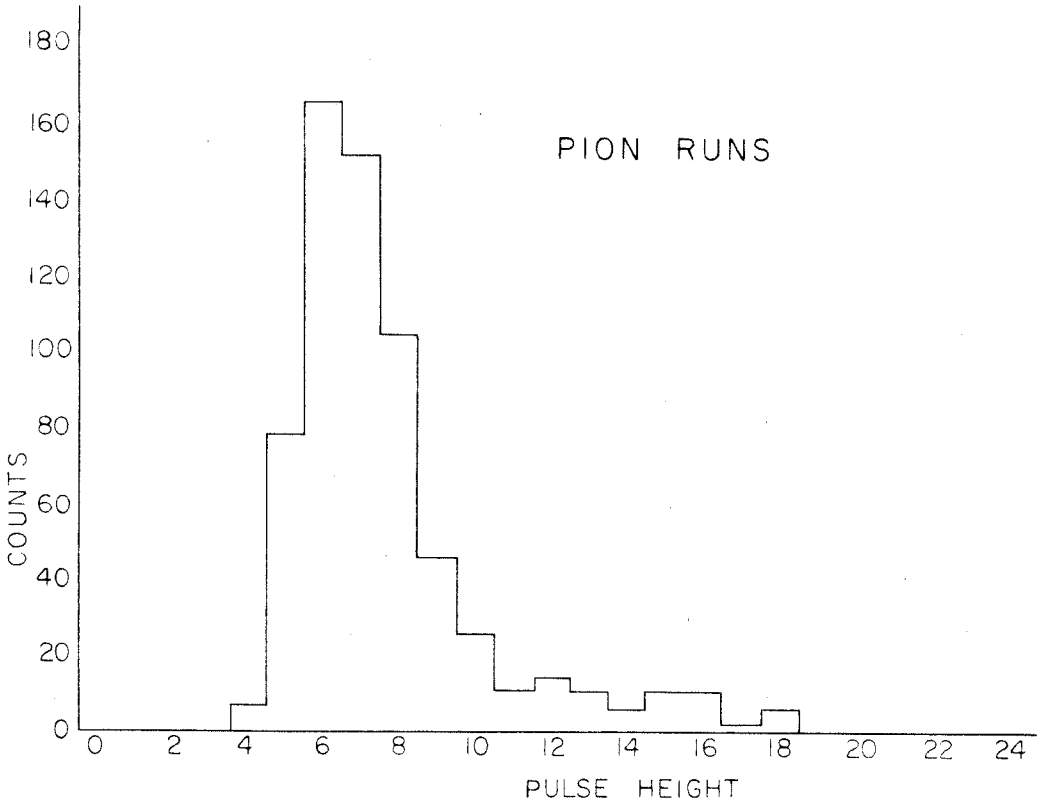
PION RUNS
COUNTS
PULSE HEIGHT
0
20
40
60
80
100
120
140
160
180
0
2
4
6
8
10
12
14
16
18
20
22
24

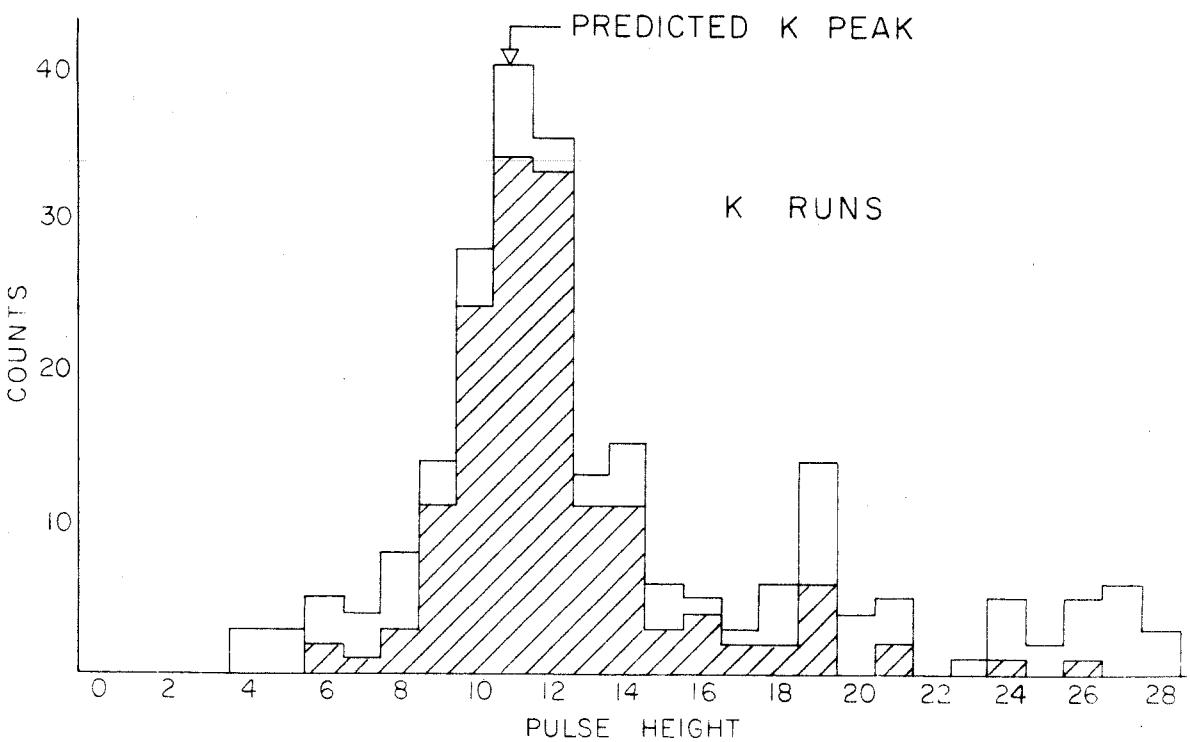
PREDICTED K PEAK
K RUNS
COUNTS
PULSE HEIGHT
10
20
30
40
0
2
4
6
8
10
12
14
16
18
20
22
24
26
28

FIGURE 20

SINGLE COUNTER SPECTRUM

The spectrum of pulse heights from C-3 on a K run with P_o = 422 is shown. The events indicated by cross hatching are those that are identified as K mesons by their pulse height in C-1 and C-2.

The Čerenkov counter was not working as efficiently for this run as it was when the data of figures 17-19 were taken, and consequently a pion peak appears in the spectrum. However, the K peak is still clearly visible.

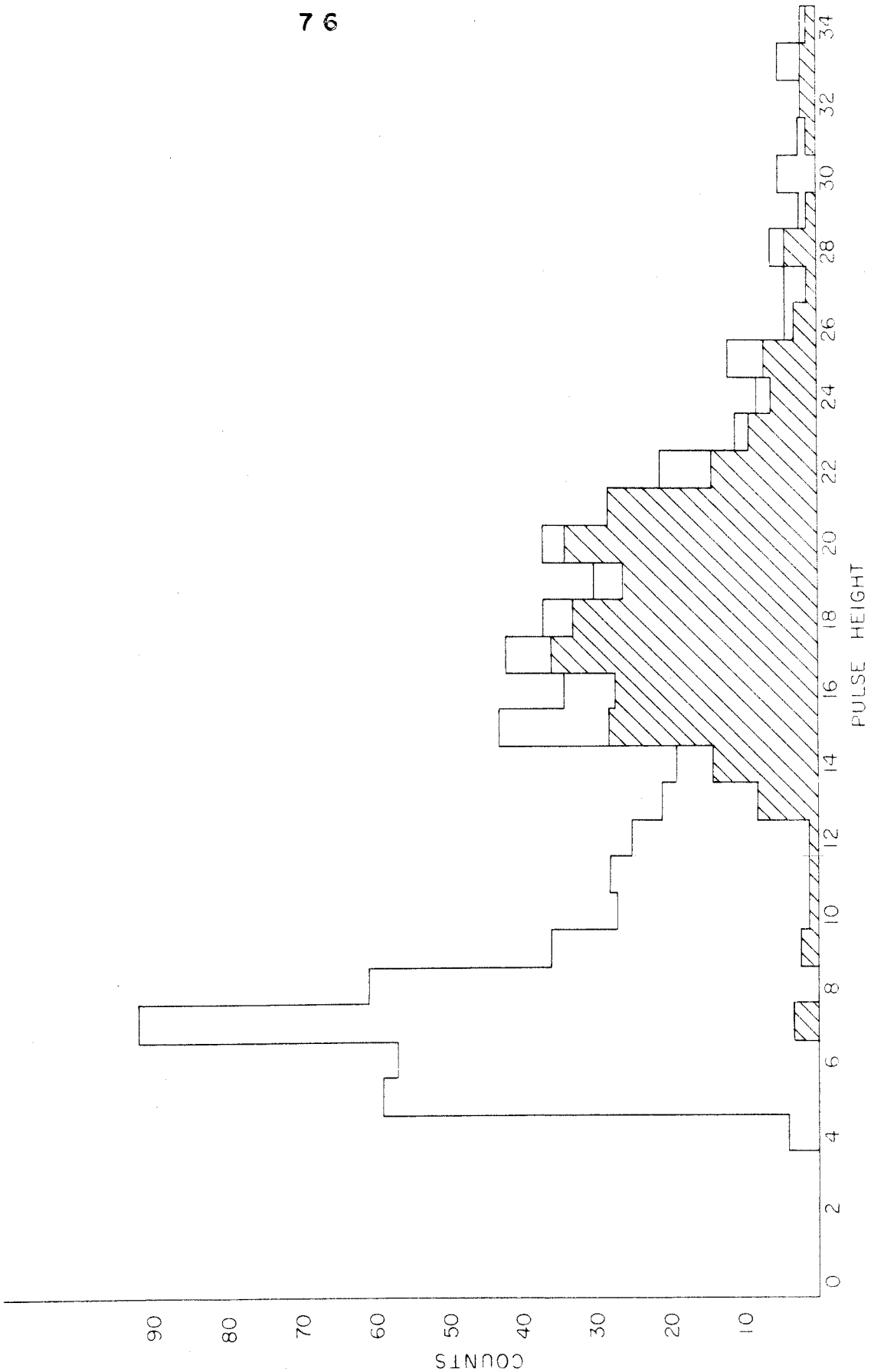
COUNTS
90
80
70
60
50
40
30
20
10
0
2
4
6
8
10
12
14
16
18
20
22
24
26
28
30
32
34
PULSE HEIGHT

taken. For the momenta selected, the ratio of protons to K's was 2000 to 1, but these are all stopped by the lead absorber before entering the last counter. The trouble arose from protons whose momenta were higher than that for which the magnet was set and there might have been as many as 10,000 of these entering the aperture per K meson counted since the $\frac{\Delta P}{P}$ was not restricted to 10 %.

B. Backgrounds

To determine the K counting rate from hydrogen, the empty target runs were subtracted from the full target runs. This was in contrast to the procedure of Donoho and Walker where the below threshold runs were subtracted. In that experiment, the geometry was such that very little of the target material was seen. There was also the possibility of identifying pions and protons as K mesons, and since the pion and proton counting rates did not change appreciably when the synchrotron energy was lowered below the K threshold, these runs were used as backgrounds.

In this experiment a great deal of the target walls and air path was seen and consequently the empty target runs must be subtracted. The below threshold runs that were taken have a number of K mesons that was consistent with an estimate of production in the target walls due to the motion of the nucleons in the nucleus.

The use of the Čerenkov counter and the antiscattering devices have reduced the pion and proton contamination considerably, and the errors made, due to erroneously identifying pions and protons as K

mesons, were estimated to be much less than the statistical accuracy of the points obtained.

In order to verify this, both full and empty target runs should have been taken below threshold, but it was felt that the machine time could be more profitably spent.

The number of K mesons appearing in the empty target runs was somewhat higher than might be expected on the basis of the ratio of protons of target material in the beam, to liquid H_2 in the beam. This might be accounted for by including an estimate of the Σ K reactions possible, due to the nucleon motion in the target material. In the case of the Σ reactions, the protons contributed to the $\gamma + p \rightarrow \Sigma^0 + K^+$ reaction and in addition the neutrons yielded K's from the $\gamma + n \rightarrow \Sigma^- + K^+$ reaction.

When data were obtained at 25° and a momentum of 422 MEV/C the peak photon energy of the beam was 1080 MEV. At this angle and momentum it would require a photon of 1135 MEV to obtain K^+ mesons in association with Σ hyperons from hydrogen. In a complex nuclei, a nucleon momentum antiparallel to the photon beam of 100 MEV/C or 50 MEV/C would reduce the photon energy needed to 1030 or 1070 MEV respectively.

C. Counting Rates

The K^+ counting rates for the full and empty target runs are shown in Table 5.

TABLE 5

K COUNTING RATES

K	θCM	θlab	Target	K^+ Counted	BIPS	Net Counts/100 BIPS
1000	28.5	10°	H_2	136	7911	1.72 ± .147
			MT	25	4729	.53 ± .106
						1.19 ± .18
1000	72	25°	H_2	128	17,614	.728 ± .064
			MT	8	9,146	.088 ± .031
						.64 ± .071
			H_2	386	32,567	1.19 ± .06
			MT	23	9,608	.24 ± .05
						.95 ± .078
1065	40	10°	H_2	180	9,591	1.88 ± .14
			MT	20	3,000	.66 ± .148
						1.22 ± .20
953	35	10°	H_2	115	8,000	1.44 ± .136
			MT	9	2,163	.42 ± .139
						1.02 ± .19

Table 6 gives the counting rates for scattered protons when the narrow aperture counter was used and in addition lists the data taken below the $K^+ \Lambda^o$ threshold. Since protons from the H_2 which pass through the narrow aperture counter cannot hit the pole pieces, the numbers of scattered protons should be the same for the three conditions listed.

The counting rate for the one Σ point was obtained by subtracting from the 1115 MEV net counting rate, the net counting rate at 1030 MEV multiplied by the ratio of the n(k) factors for the two energies. The ratio goes as $\frac{W_\Sigma}{W_\Lambda} \frac{E_\Lambda}{E_\Sigma} = \frac{1090}{1063} \frac{1025}{1115} = .943$.

Making this correction to the data:

E_o	K^+ counts per 100 bips
1115	$1.22 \pm .20$
1025	$(1.02 \pm .19) \times .943 = .96 \pm .18$
net counting rate	$.26 \pm .27$

TABLE 6

COUNTING RATES FOR K's BELOW THRESHOLD AND SCATTERED PROTONS

E_o	lab	P	Target	BIPS	100 K/BIP	Scattered Protons / 100 BIP
1080	10^o	514	H_2	7911	$1.72 \pm .147$	$1.01 \pm .11$
1080	10^o	514	MT	4729	$.53 \pm .106$	$.92 \pm .14$
900	10^o	514	H_2	3114	$.25 \pm .09$	$.68 \pm .15$
1080	25^o	420	H_2	17614	$.728 \pm .064$	$.181 \pm .03$
1080	25^o	420	MT	9146	$.088 \pm .031$	$.132 \pm .04$
900	25^o	420	H_2	3266	$.00 \pm .03$	$.246 \pm .09$

V. CROSS SECTIONS AND CORRECTIONS

A. Counting Rate-Cross Section Relationship

The basic formula for relating cross section to counting rate is

$$C = \sigma(\theta) \frac{\partial \Omega'}{\partial \Omega} \Delta\Omega N \rho \bar{\ell} A\, n(k) \Delta k$$

where:

C	is counts (per 100 bips)
$\sigma(\theta)$	is C. M. (Center of Momentum) differential cross section
$\Delta \Omega$	is the solid angle of the spectrometer
$\frac{\partial \Omega'}{\partial \Omega}$	is solid angle transformation from the C. M to lab system
$\rho \bar{\ell} N$	is average number of protons per cm^2 traversed by the beam
$n(k)$	is number of photons per MEV of energy k(per 100 bips)
Δk	is the photon energy interval which contributes to production of K mesons detected
A	is a correction factor due to decays, detection efficiency, etc.

$$\Delta k = \frac{\partial k}{\partial P_o} P_o \frac{\Delta P_o}{P_o}$$

$$n(k)dk = \frac{W}{E_o} B\left(E_o, \frac{k}{E_o}\right) \frac{dk}{k}$$

$$C = \sigma(\theta)\Delta\Omega N\rho\bar{\ell}\,\frac{\Delta P_o}{P_o}\,\frac{\partial k}{\partial P_o}\,P_o\,\frac{\partial\Omega'}{\partial\Omega}\,\frac{W}{E_o}\,B\,(E_o\,\frac{k}{E_o})\,\frac{1}{k}\,A$$

$$= \sigma(\theta)\Delta\Omega N\rho\bar{\ell}\,\frac{\Delta P_o}{P_o}\,\beta^2 P_o\,G(P_o, k)\,\frac{W}{E_o}\,B(E_o, \frac{k}{E_o})\,\frac{1}{k}\,A$$

where

$$G(P_o, k) \equiv \frac{1}{\beta^2}\,\frac{\partial k}{\partial P_o}\,\frac{\partial\Omega'}{\partial\Omega}$$

G is a slowly varying function of k for a given P_o; and a very slowly varying function of P_o for a given k .

The formulas are put into this form for ease in comparing cross sections and counting rates, since the counting rate for a given cross section depends very nearly on $P\beta^2$ alone, if corrected for decay. The values of G and $P_o\beta^2$ come from the kinematics of the reaction and once the angle and momentum are fixed, their values are determined.

The values for ρ, the density of liquid hydrogen is .0703 gm/cm^3 (16) in equilibrium with its own vapor at a pressure approximately two pounds greater than atmospheric. N is Avogadro's number and the value of $\bar{\ell}$, the average length of target traversed by the beam, is 7. 23 cm.

The values of $\frac{W}{E_o}\,B\,(E_o\,\frac{k}{E})\,\frac{1}{k}$ come from the work of Gomez (9) on the energy calibration of the beam and Walker et al. (8) on the measurement of the photon spectrum, as mentioned in

section III.

B. Decay Correction

With the long flight path, the relatively low particle velocities and the short K^+ life time encountered in this experiment, the decay correction was extremely large. The flight path has been broken up into two sections, one before the aperture counter and one after it, to compute the correction. The correction factor is $R = e^{-\frac{205}{P^*}} \times e^{-\frac{351}{P_o}}$ where

P_o is the momentum in the magnet

P^* is the momentum before the aperture counter

K lifetime = 1.22×10^{-8} sec. (17)

In calculating the decay correction the distance used was foci to foci and this lead to certain difficulties. It is now attempted to list these troubles and estimate the corrections required. There were three separate sources of trouble.

1. K particles which pass through the system, decay after the second focus, and whose decay products produce signals in the counters such that the event was not considered a K meson.
2. K particles which would have been counted had they not decayed, but whose decay products pass through the system in such a manner that they appeared to be K mesons.

3. K mesons which, because of the wrong momenta or direction, would not have been counted, but whose decay products pass through the system in such a manner that they appeared to be K mesons.

Case 1 would tend to decrease the observed K counting rate while cases 2 and 3 tended to increase the counting rate.

To reduce the effects of Case 1, all lead and other material were removed from behind the final counter. This allowed the K's to pass out of the counter housing and not stop close to the counter. The decays would then, on the average, take place at a much larger distance from the rear counter and the probability of a decay product coming back through the counter was quite small.

Decays that occurred in flight after the focus could produce either a larger or smaller pulse height, depending upon the decay mode and the direction. This effect was estimated as being very small and, in fact, an upper limit was set by the fraction of events which are K-like in C-1 and C-2 and that were thrown out by the C-3 pulse being too large or small.

The effects of cases 2 and 3 were quite small because the large energies available in the decay of the K meson tended to give the decay products a high velocity in the forward direction which triggered the Čerenkov counter or lower velocities at angles so large that they had little chance of striking the counters.

An estimate of this has been made in the following manner. At the lowest momentum (425 MEV/C) run in these experiments, no

changed particles of momenta under 300 MEV/C could pass through the aperture counter and the rear counters (without a scattering). At momenta of 300 MEV and above, the Čerenkov counter was very efficient for both π and μ mesons and consequently any K decay occurring before the aperture counter would be vetoed or ruled out in the pulse height analysis.

This reduced cases 2 and 3 to only those K mesons which passed through the aperture counter.

The peak energy of the machine was set so that the K mesons observed had nearly the highest possible momentum obtainable at a given angle, and consequently case 3 was again restricted.

Approximately 40 $^{o}/_{o}$ of the K mesons of the correct momentum decayed before entering the magnet. At lower momenta this fraction rose and the cross section and the various kinematic factors determining counting rate fell. Consequently only K particles passing through the aperture counter with a momentum close to that for which the magnet was set need be considered. The region between the counters and the magnet in which a decay product passing through the counters could originate, was subdivided into 24 smaller regions. Each region was assigned a weight determined by the probability of a K meson decaying in that region. The probability of a decay product originating at the center of each region and passing through the counters in such a manner as to be identified as a K was then calculated for each possible decay mode.

The K_β mode of decay was eliminated because any electron with sufficient range to reach the third counter would trigger the Čerenkov counter.

The two principal decay modes $K_{\mu 2}$ (58.8 °/o) and $K_{\pi 2}$ (25.6 °/o) and the $K_{\mu 3}$ (4 °/o) produced charged secondaries with a center of momentum velocity greater than the K meson velocity in the lab. The result was that if the charged particle was to have a $\beta < .9$ in the lab it had to make an angle (lab) with the original K direction so large that it was extremely unlikely to pass through all four of the counters.

The remaining two decay modes were three body decays having less energy available and did contribute a small amount.

However, some care had to be taken with these two modes ($K \longrightarrow \pi^+ + \pi^+ + \pi^-$ and $K \longrightarrow \pi^o + \pi^o + \pi^+$) that the second charged particle did not also go through the counters or one of the γ rays from a π^o did not convert in the lead absorber and give too large a pulse in the third counter.

A correction of less than 1 °/o was necessary to account for these processes occurring from all momenta K mesons decaying after the magnet and judging by the manner in which the rate changed as the particles decayed closer to the magnet, about a 1 °/o correction was required for decays occurring in the magnetic field.

C. Other Corrections

The Čerenkov counter vetoed a certain fraction of the K mesons passing through it and for the first set of runs it was estimated to be

5 °/o. For the second series of runs, less gain was employed in the circuitry and the efficiency for $\beta = .7$ particles was measured to be less than $2\frac{1}{2}$ °/o.

The nuclear absorption was calculated, using a value of 10 millibarns (18) for the interaction cross section. The per cent absorption for various materials is listed below:

$\frac{1}{2}$" lead	1.4 °/o
1" carbon	1.0 °/o
counters	4 °/o

One half inch of lead was used in all cases and in addition, a one inch piece of carbon was used for the 514 MEV/C point.

During the first series of runs, the absorbers used were not placed immediately in front of the last counter and a fraction of the mesons could be scattered out. For the 10° point this correction amounted to 4 °/o, while at the 25° point, this was a 3 °/o correction.

The change in $\frac{\Delta P}{P}$ due to the energy loss in the aperture counter has been determined to be:

2 °/o for the 420 MEV/C runs

$1\frac{1}{2}$ °/o for the 510 MEV/C run

In order to fit four counters in the counter housing, it was necessary to move the position of the focus counter back from the focus position, and move the first counter slightly forward. These changes tended to lower the counting rate by $3\frac{1}{2}$ °/o principally by reducing the $\frac{\Delta P}{P}$ acceptance of the spectrometer. These two

effects reduce the $\frac{\Delta P}{P_o}$ from .10 to .0945 and .0950 for the 420 MEV/C and 514 MEV/C runs respectively.

D. Cross Sections

The first part of Table 7 lists the various kinematic factors for the reactions studied. Below that are listed several measured or calculated factors which entered into the calculation of the cross sections and the values obtained for the cross sections.

TABLE 7

CROSS SECTIONS

Reaction	Λ	Λ	Λ	Λ	Σ°
θlab	10	25	25	10	10
P_o(MEV/C) in magnet	514	420	422	422	422
P^*(MEV/C) at target	519.5	426.5	428.5	428.5	428.5
k(MEV)	1000	1000	1000	953	1073
E_o(MEV)	1072	1072	1080	1025	1115
θ C. M. system	28.5	72	72	35	40
T(MEV) of K^+ in C. M. system	35.7	35.7	35.7	17.2	13
G	8.52	8.43	8.40	11.50	13.80
$\Delta\ \Omega$ (ster.)	.00408	.00408	.00619	.00619	.00619
K decay (corrected)	.347	.273	.275	.275	.275
Time of flight efficiency	.87	.87	.85	.85	.85
Net K^+ count/100 bips	1.19±.18	.64±.071	.95±.078	1.22±.20	.26±.27
$\frac{d\sigma}{d\Omega}$ x 10^{-31} cm^2/ster.	1.55±.23	1.52±.175	1.47±.12	1.12±.20	.33±.34

VI. THEORY

Various authors (19) have attempted to analyze the photoproduction of K mesons near threshold by means of a perturbation approach. They have predicted the expected angular distributions and excitation functions for scalar and pseudoscalar mesons with several different magnetic moments assigned to the hyperon. Even though there is considerable doubt as to the validity of perturbation theory as applied to this case, certain aspects of the work may prove valuable in interpreting the data.

In a manner analogous to the low energy pion analysis, Feld, considering S and P waves only, has written the differential cross section for scalar K mesons as

$$\frac{d\sigma}{d\Omega} = \left|M_1 + (E_1 - E_3 + M_3')\cos\theta\right|^2 + \tfrac{1}{2}\left\{\left|E_1 + 2E_3\right|^2 + \left|E_1 - E_3 - M_3'\right|^2\right\}\sin^2\theta$$

where M, E, M' and E' are amplitudes corresponding to magnetic and electric dipole and quadrupole photons and the subscripts are twice the angular momentum. (For the pseudoscalar case the M and E are interchanged.)

The electric dipole absorption is spin independent and $E_1 = E_3$. Hence for scalar mesons, the $\cos\theta$ interference term can be neglected to the extent that magnetic quadrupole may be neglected. The pseudoscalar case, having spin-dependent magnetic dipole terms in the interference, should have a strong $\cos\theta$ appearance barring

some accidental cancellation. This $\cos\theta$ term present in the pseudoscalar case and absent for the scalar case is quite apparent in the results obtained by Marshak and Fujii, Moravcsik and Kawaguchi, and Feld and Costa (19).

There is the possibility that the angular distributions will be of a form such that there is no interference because the reaction is caused by absorption of a single multipole. In this case the multipole can be identified by examining the angular distribution, excitation function and knowing the parity (see Table 8). Conversely, the parity can be determined once the L and J values are assigned if the multipole causing the reaction can be labeled as electric or magnetic.

Thus by looking at the process $\gamma + n \longrightarrow K^o + \Lambda^o$ where there is no E_1 or E_3, and comparing it with $\gamma + p \longrightarrow K^+ + \Lambda^o$ where both M and E are possible, it may be possible to determine the relative K parity. Unfortunately, this is a very difficult experiment, and it also assumes that the K^+, K^o parity is positive, an assumption that recently has received theoretical attention (20).

The $K\Sigma$ presents a somewhat similar situation, only here some of the experimental work can be done with the existing techniques and the K^oK^+ parity does not enter.

There are four possible reactions,

$$\gamma + p \longrightarrow \Sigma^o + K^+$$
$$\gamma + p \longrightarrow \Sigma^+ + K^o$$
$$\gamma + n \longrightarrow \Sigma^- + K^+$$
$$\gamma + n \longrightarrow \Sigma^o + K^o$$

TABLE 8

MULTIPOLE ABSORBTION AND POSSIBLE K STATES

Photon Absorbed	State	Angular Distribution	Scalar Case ℓ	Scalar Case K	Scalar Case State	Scalar Case P Dependence	Pseudoscalar Case ℓ	Pseudoscalar Case K	Pseudoscalar Case State	Pseudoscalar Case P Dependence
Electric Dipole	1/2-	constant	1	1	$P_{1/2}$	P^3	0	0	$S_{1/2}$	P
	3/2-	$2+3\sin^2\theta$	1	1	$P_{3/2}$	P^3	2	2	$D_{3/2}$	P^5
Magnetic Dipole	1/2+	constant	0	0	$S_{1/2}$	P	1	1	$P_{1/2}$	P^3
	3/2+	$2+3\sin^2\theta$	2	2	$D_{3/2}$	P^5	1	1	$P_{1/2}$	P^3
Electric Quadrupole	3/2+	$1+\cos^2\theta$	2	2	$D_{3/2}$	P^5	1	1	$P_{3/2}$	P^3
	5/2+	$1+6\cos^2\theta-5\cos^4\theta$	2	2	$D_{5/2}$	P^5	3	3	$P_{5/2}$	P^7
Magnetic Quadrupole	3/2-	$1+\cos^2\theta$	1	1	$P_{3/2}$	P^3	2	2	$D_{3/2}$	P^5
	5/2-	$1+6\cos^2\theta-5\cos^4\theta$	3	3	$F_{5/2}$	P^7	2	2	$D_{5/2}$	P^5

which may be examined under electric dipole absorption. Using charge independence, the Clebsch - Gordan coefficients give

$$p \rightleftharpoons (1/3)^{\frac{1}{2}} \Sigma^{o} K^{+} + (2/3)^{\frac{1}{2}} \Sigma^{+} K^{o}$$

$$n \rightleftharpoons (2/3)^{\frac{1}{2}} \Sigma^{-} K^{+} + (1/3)^{\frac{1}{2}} \Sigma^{o} K^{o}$$

In a manner similar to the work on the π^{-}/π^{+} ratio from deuterium, a classical argument is used to obtain the effective dipole moment by including the nucleon current from recoil as well as the meson current term. The results are as follows where p is the effective electric dipole moment matrix element.

$$p^2 (\Sigma^{o} K^{+}) \cong 1/3\ (1) = .33$$

$$p^2 (\Sigma^{+} K^{o}) \cong 2/3 \left(\frac{M_K}{M_\Sigma}\right)^2 = 0.115$$

$$p^2 (\Sigma^{-} K^{+}) \cong 2/3 \left(1 + \frac{M_K}{M_\Sigma}\right)^2 = 1.33$$

$$p^2 (\Sigma^{o} K^{o}) \cong 1/3 \cdot O = O$$

(M_K and M_Σ are the masses of the K meson and the Σ hyperon respectively.)

This means that K^{+} production off neutrons is enhanced by a factor of 4 over $K^{+}\Sigma^{o}$ production from protons, for electric dipole production. If the production is magnetic dipole, this ratio of 4 to 1 is quite unlikely but not impossible, due to the unknown hyperon magnetic moments.

Unlike pion physics where there is a close correspondence between scattering and photoproduction, strange particle photoproduction does not proceed through the same states as scattering. The isotopic spin assignment in the photoproduction of a K with a Λ^o is $\frac{1}{2}$, while the K with Σ's can be either $\frac{1}{2}$ or 3/2. With K scattering, since one does not scatter K's off hyperons, but nucleons, the isotopic spin assignments are 0 and 1.

In addition, the elastic scattering of charged K mesons off protons involves a mixture of both the Σ and Λ hyperon states, while the K neutron scattering is purely through the Σ states.

The reactions analogous to K photoproduction are

$$\pi^+ + n \longrightarrow K^+ + \Lambda^o$$

$$\pi^+ + n \longrightarrow K^+ + \Sigma^o$$

and they have the same final states as the reaction studied in this experiment. The data on pion production of strange particles are obtained predominantly with bubble chambers, so at present the statistical accuracy is quite poor.

It has been pointed out by Mathews and Salam (21), Goebel (22), and Barshay (23), that the K hyperon parity can be determined from scattering data. Mathews and Salam, using dispersion theory and assuming the $\Sigma\ \Lambda^o$ parity is even, claim that since the K^+ scattering data are isotropic and energy independent with a repulsive potential, the KY^o parity will be scalar if the K^-p scattering is repulsive, and

pseudoscalar if the K^-P scattering is attractive.

Barshay, without assuming the $\Sigma\Lambda$ parity as being even, has shown that if the K^- scattering is attractive, they are indeed even and the K is pseudoscalar. If the scattering is repulsive, the other three possible permutations of the $K\Sigma\Lambda$ parities are possible and the scattering of K mesons off neutrons must be done to determine the $K\Sigma$ parity.

Gell - Mann (25) has investigated a model of strong couplings where the pion is coupled equally to every baryon, while the K interactions can be characterized by four separate coupling constants. It is proposed to determine the constants $g_{\Lambda K}$ and $g_{\Sigma K}$ from the photoproduction data, hence no prediction of the relative $\Lambda\Sigma$ yield can be made. Gell - Mann predicts that the single pion coupling is very strong, while the K couplings are moderately strong. Using this model of global symmetry, it is possible to predict the Λ^0 and Σ^0 magnetic moments and the transition moment μ_T between them. The Λ^0 and Σ^0 magnetic moments then come out zero, to the extent to which the K interactions can be neglected, due to the charge symmetry of the π, Λ and Σ multiplets.

Adair (26) has analyzed the pion and photoproduction of strange particles. He predicts that if the Λ and Σ have the same parity the Λ cross section will exhibit a cusp at the threshold for the Σ production and that information about the K parity may be extracted by examining the behavior around this cusp. He also finds that the pion production of strange particles is 1/3 to 1/2 of the

maximum allowable by conservation laws, and perhaps the K coupling constant is not small.

Feld (27) points out that there is some evidence that strange particle production is occurring through a resonant state. The cross section for pion produced Λ^{o}'s rises rapidly above threshold and then follows a curve like the total $\pi^{-}p$ cross section, which appears to have a resonance.

VII. RESULTS AND CONCLUSIONS

The results obtained in this experiment do not show the marked peaking of the cross section at 70° C. M. (Center of Momentum) that was present in the data of Donoho and the early Cornell work. The cross sections obtained at 28.5° and 72° are the same well within the statistical accuracy of the experiment. The data at 1000 MEV of Donoho, this experiment, a point obtained by Wales and Sands (24) and the revised Cornell cross sections are shown in figure 21; the lower energy data, in figure 22.

The angular distributions are now in good agreement with an $S_{1/2}$ state which is what is predicted by the linear dependence on momentum of the cross section near threshold.

The excitation function obtained by Cornell at 85° C. M. and by Donoho at 90° C. M. have this form, and the forward angle points obtained in this experiment are also in good agreement with a linear dependence upon momentum.

If the K is produced in a $S_{1/2}$ state, and the evidence weighs heavily for it, the reaction takes place through electric dipole absorption if the K is pseudoscalar and magnetic dipole if scalar. Because of this, there seems to be little to be learned about the K parity from a detailed fitting of the data by the analysis of Marshak and Fujii, Moravcsik and Kawaguchi, or Feld and Costa. However, the K parity might be determined by investigation of the $\gamma + n^{o} \longrightarrow K^{o} + \Lambda^{o}$ reaction, as was seen in the previous section.

FIGURE 21

ANGULAR DISTRIBUTIONS AT k = 1010 and 1000 MEV

$$\gamma + p \longrightarrow K^{+} + \Lambda^{o}$$

The two points taken at 72^{o} (C. M.) in this experiment were not combined because they were obtained using different experimental configurations.

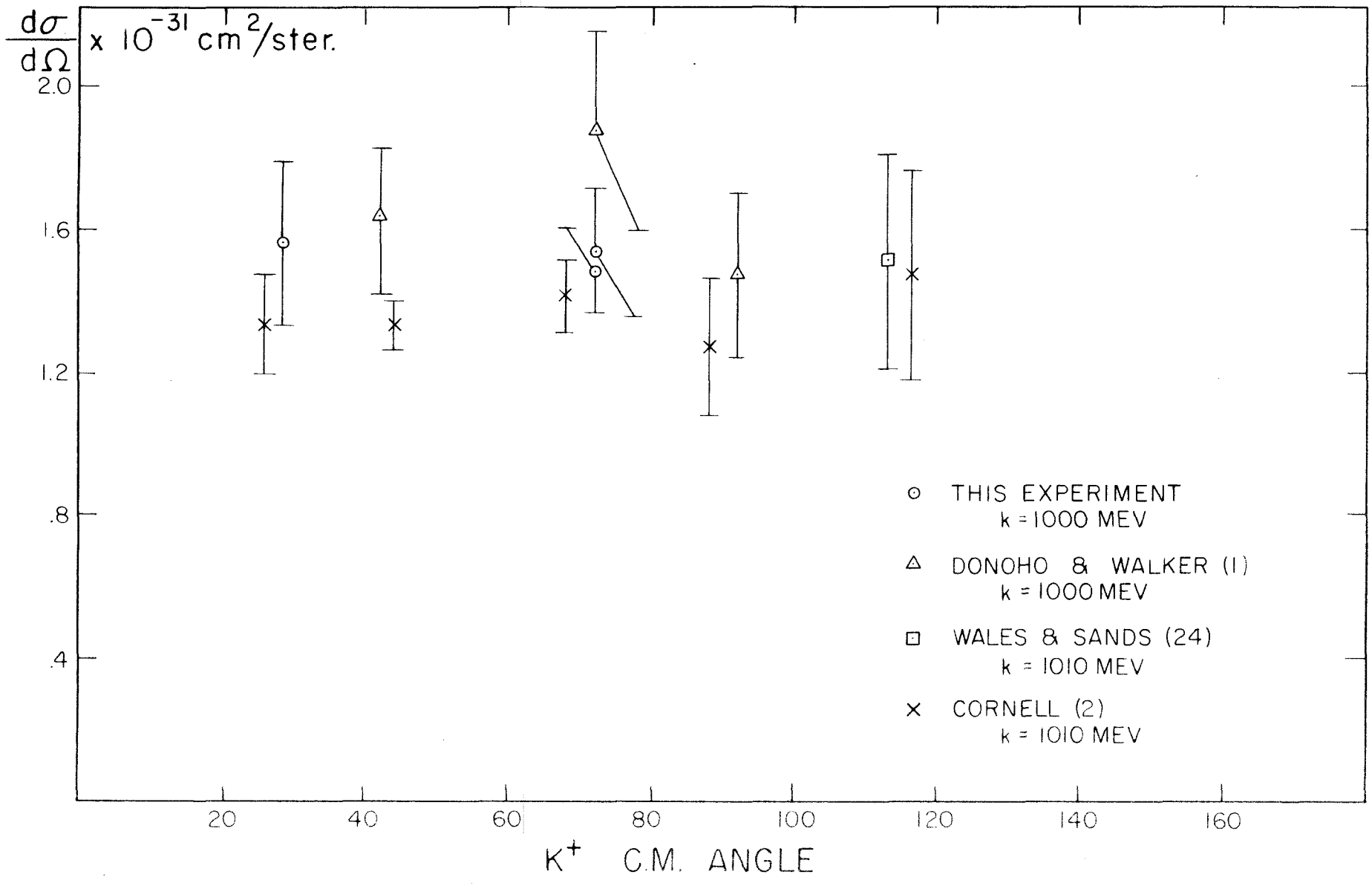
dσ/dΩ x 10^-31 cm^2/ster.
2.0
1.6
1.2
.8
.4
20
40
60
80
100
120
140
160
K+ C.M. ANGLE
THIS EXPERIMENT
k = 1000 MEV
DONOHO & WALKER (1)
k = 1000 MEV
WALES & SANDS (24)
k = 1010 MEV
CORNELL (2)
k = 1010 MEV
100

FIGURE 22

ANGULAR DISTRIBUTIONS K = 953 to k = 980 MEV

$\gamma + p \longrightarrow K^{+} + \Lambda^{o}$

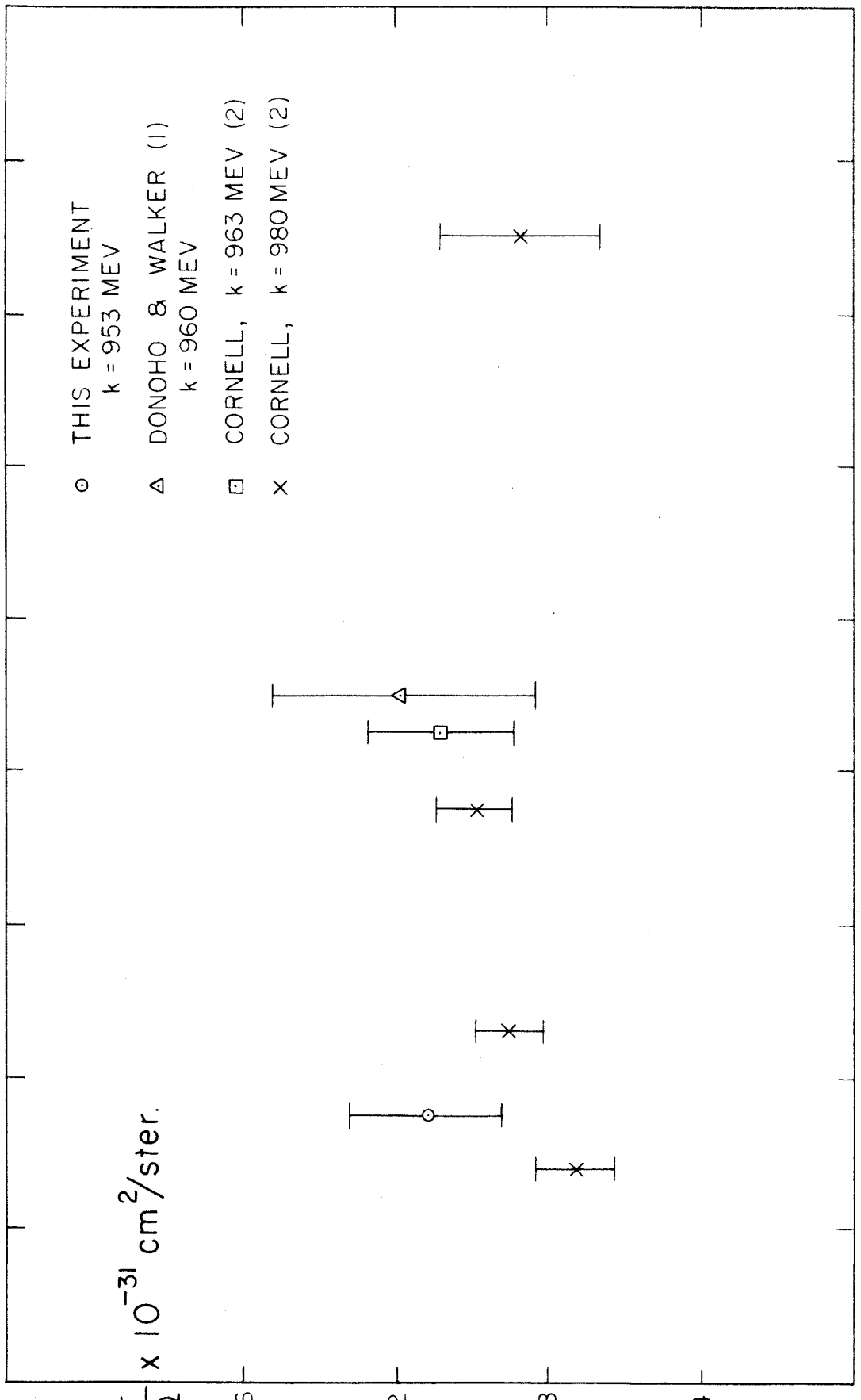
THIS EXPERIMENT
k = 953 MEV
DONOHO & WALKER (1)
k = 960 MEV
CORNELL, k = 963 MEV (2)
CORNELL, k = 980 MEV (2)
dσ/dΩ x 10^-31 cm^2/ster.
1.6
1.2
.8
.4
20
40
60
80
100
120
140
160
K+ C.M. ANGLE

The perturbation calculations can be used to obtain an estimate of the K-hyperon coupling constants. If the K is pseudoscalar, the analysis of the data leads to a small value $\frac{g^2}{4\pi} \approx 2$ as compared to the pions with $\frac{g^2}{4\pi} \approx 15$.

It is of some interest to compare the $\gamma + p \rightarrow K^+ + \Lambda^o$ data at 1000 MEV, $\frac{P_{C.M.}}{M_k C} = .4$ to the $\gamma + p \rightarrow \pi^+ + n^o$ data at 167 MEV, $\frac{P_{C.M.}}{M_\pi C} = .4$. In both cases the excitation function is still rising linearly with the C. M. momentum, but deviates very soon-the π^+ rising into the 3/2 3/2 resonance, the K^+ leveling off. In both cases the angular distribution of the mesons in the C. M. is isotropic--the values of the B and C coefficients in an $A + B \cos\theta + C \cos^2\theta$ analysis of the π^+ data being 1/10 the A value.

It appears quite unlikely that the reaction $\gamma + p \longrightarrow K^+ + \Lambda^o$ is dominated by a resonance near 1000 MEV. Judging from the angular distributions obtained by F. P. Dixon (28) for the reaction $\gamma + P \longrightarrow \pi^+ + n$, a rather high angular momentum state would be involved in a "resonance" which would begin near 1000 MEV photon energy and this would be completely incompatible with the isotropy exhibited by the K^+ and Λ^o.

The cross section obtained for the Σ^o reaction has an error of a magnitude so large that it may mask any significance that the data may have. When this point was planned it was hoped that the Σ cross section would be as large as the corresponding Λ^o cross section and that the empty target runs would contribute about 20 °/o of the full target rate, not 30 °/o. This would have led to a result with

approximately a 40 °/o statistical error.

Even with this large error, it can be seen that the $\Sigma^{o} K^{+}$ cross section is smaller than the $\Lambda^{o} K^{+}$ cross section at the same C. M. momentum. The one Cornell (2) point also shows this result to be true.

The one Σ point at each institution is compared in table 9.

TABLE 9

COMPARISON OF CALTECH AND CORNELL DATA ON

$\gamma + p \longrightarrow K^{+} + \Sigma^{o}$ REACTION

	Caltech	Cornell
k	1073	1111
θ C. M.	40^{o}	85^{o}
P C. M. (MEV/C)	114	167
$\frac{d\sigma}{d\Omega}$ x 10^{-31} cm^{2}/ster	$.33 \pm .34$	$.61 \pm .17$
$\frac{d\sigma}{d\Omega}$ x 10^{-31} cm^{2}/ster for $K\Lambda^{o}$ at same C. M. Momenta	$\sim .85$	~ 1.0

It must be noted that the total Σ - K production from protons is somewhat higher because of the competing reaction $\gamma + p \longrightarrow K^{o} + \Sigma^{+}$. If the K Σ production arises from a final state interaction or an intermediate state, isotopic spin will predict the $\Sigma^{o} K^{+}$ to $\Sigma^{+} K^{o}$

ratio to be 1:2 and 2:1 in the $T = \frac{1}{2}$ and 3/2 states respectively. If however, the reaction proceeds directly Feld predicts a ratio of 3:1.

Unfortunately due to the low cross sections, the data on strange particle photoproduction are difficult to obtain and have poor statistical accuracy. With the Σ° reaction the difficulty is compounded by the necessity of subtracting comparable numbers to eliminate the Λ° contributions, and to obtain information about the production of K^{+} mesons from neutrons a third subtraction will have to be done.

At higher photon energies and higher momentum particles in the lab system, the counting rates should increase due to kinematic factors and less K^{+} mesons decay in flight. However, the detection will become more difficult as the K velocity approaches the pion velocity for a given momentum.

APPENDIX

A preprint has recently been received of a paper by R. H. Capps entitled "Photoproduction of K Mesons and K-Hyperon Parities." This paper deals with the subject through perturbation theory, making an angular momentum analysis and calculating the results using the magnetic moments of the hyperons predicted by global symmetry. However, the long wave length approximation of Feld and Costa is not made in this work because of the high energies involved.

It is interesting to note some of the conclusions that can be drawn. Assuming $(g_{\Sigma}/g_{\Lambda}) = 1$ (which is reasonable on the basis of the photoproduction evidence) and assuming the Σ^{o} and Λ^{o} magnetic moments are zero and their transition moment $\mu_{t} = 1.8$ nuclear magnetons, (from global symmetry) the experimental data on the $K^{+}\ \Lambda^{o}$ production fit very well for $g_{\Sigma}/g_{\Lambda} = -1$ and poorly for $g_{\Sigma}/g_{\Lambda} = +1$ for both a scalar and pseudoscalar K meson. However, this is not to be interpreted as experimental evidence for these values of the magnetic moment.

The value of g_{Σ}/g_{Λ} can be said to be negative to the extent that perturbation theory for this case and the magnetic moments predicted by global symmetry are believed.

There is one very striking difference between this work and the work of Feld and Costa (19). This concerns the ratio of K^{+} production off neutrons and protons via the reactions $\gamma + n \longrightarrow K^{+} + \Sigma^{-}$ and $\gamma + P \longrightarrow K^{+} + \Sigma^{o}$. Again using the magnetic moments obtained from global symmetry, and the value $g_{\Sigma}/g_{\Lambda} = -1$ obtained from the

K Λ^{o} data, the ratio $K^{+}\Sigma^{-}$ to $K^{+}\Sigma^{o}$ is 16 to 1 if the K is pseudoscalar and it is around 1 to 6 if the K is scalar.

REFERENCES

1. Donoho, P. L., Thesis, California Institute of Technology, (1957).

   Donoho, P. L. and Walker, R. L., Phys. Rev., 112, 981 (1958).

2. Mac Daniel, B. D., Silverman, A., Wilson, R. R. and Cortellessa, G., Phys. Rev. Letters 1, 109, (1958), revised Phys. Rev. Letters, 1, 263, (1958).

3. Lattes, Occialini and Powell, Nature, 160, 453, (1947).

4. Pais, A., Phys. Rev., 86, 663, (1952).

5. Gell - Mann, M., Phys. Rev., 92, 833, (1953).

   Nakano, T. and Nishijima, K., Prog. Theor. Phys., 10, 581, (1953).

6. Glaser, Good and Morrison, "1958 Annual International Conference on High Energy Physics at CERN," p. 273.

7. Marshak, Okubo and Sudarshan, Phys. Rev., 106, 599, (1957).

   Gell - Mann, M., "1958 Annual International Conference on High Energy Physics at CERN," p. 162.

8. Donoho, Walker and Emery, private communication.

9. Gomez, R., private communication.

10. Wilson, R. R., Nuclear Inst., 1, 101, (1957).

11. Donoho, P. L., "A Magnetic Spectrometer for Analysis of Particles of Momentum Up to 1200 MEV/C," California Institute of Technology, (1957), unpublished.

12. Rossi, B., "High Energy Particles," (1952), pp. 33-34.

13. Marshall, Annual Rev. of Nuc. Sci., 4, 141, (1954).

14. Rossi, B., "High Energy Particles," (1952), pp. 15-16.

15. Wenzel, W. A., U. C. R. L., 8000, (1957).

16. Woolley, Scott and Brickwedde, Journal of Research of the National Bureau of Standards, 41, 453, (1948).

17. Gell - Mann and Rosenfeld, Annual Rev. of Nuc. Sci., 7, 411, (1957).

18. Puppi, G., Proceedings of the Seventh Rochester Conference, (1957).

19. Moravcsik, M. J. and Kawaguchi, M., Phys. Rev., 107, 563, (1957).

Fujii, A. and Marshak, R. E., Phys. Rev., 107, 570, (1957).

Feld, B. T. and Costa, G., Phys. Rev., 110, 968, (1958).

20. Pais, A., Phys. Rev., 112, 624, (1958)

21. Mathews and Salam, Phys. Rev., 110, 569, (1958).

22. Goebel, C., Phys. Rev., 110, 572, (1958).

23. Barshay, S., Phys. Rev. Letters, 1, 177, (1958).

24. Wales, W. and Sands, M., private communication.

25. Gell - Mann, M., Phys. Rev., 100, 1296, (1957).

26. Adair, R., Phys. Rev., 111, 632, (1958).

27. Feld, B. T., "1958 Annual International Conference on High Energy Physics at CERN," p. 158.

28. Dixon, F. P. and Walker, R. L., Phys. Rev. Letters, 1, 458, (1958).